Journal of Medicinal Chemistry

ARTICLE

pubs.acs.org/jmc

Synthesis, Biological, and Antitumor Activity of a Highly Potent 6-Substituted Pyrrolo[2,3-*d*]pyrimidine Thienoyl Antifolate Inhibitor with Proton-Coupled Folate Transporter and Folate Receptor Selectivity over the Reduced Folate Carrier That Inhibits β-Glycinamide Ribonucleotide Formyltransferase

Lei Wang,[†,▽] Sita Kugel Desmoulin,[§,∥,▽] Christina Cherian,[‡] Lisa Polin,[‡,∥] Kathryn White,[‡,⊗] Juiwanna Kushner,[‡,⊗] Andreas Fulterer,[○] Min-Hwang Chang,[○] Shermaine Mitchell-Ryan,[§,∥] Mark Stout,[#] Michael F. Romero,[○] Zhanjun Hou,[‡,∥] Larry H. Matherly,[*,§,⊥,∥,‡,▽] and Aleem Gangjee[*,†,▽]

[†]Division of Medicinal Chemistry, Graduate School of Pharmaceutical Sciences, Duquesne University, 600 Forbes Avenue, Pittsburgh 15219, Pennsylvania 15282, United States

[‡]Developmental Therapeutics Program, Barbara Ann Karmanos Cancer Institute, 110 East Warren Avenue, Detroit, Michigan 48201, United States

[§]Cancer Biology Graduate Program, Wayne State University School of Medicine, Detroit, Michigan 48201, United States

[∥]Department of Oncology, Wayne State University School of Medicine, Detroit, Michigan 48201, United States

[⊥]Department of Pharmacology, Wayne State University School of Medicine, Detroit, Michigan 48201, United States

[⊗]Department of Internal Medicine, Division of Hematology-Oncology, Wayne State University School of Medicine, Detroit, Michigan 48201, United States

[○]Physiology & Biomedical Engineering, Mayo Clinic College of Medicine, Rochester, Minnesota 55905, United States

[#]Department of Pediatrics, Children's Hospital of Michigan, Detroit, Michigan 48201, United States

Supporting Information

ABSTRACT: 2-Amino-4-oxo-6-substituted pyrrolo[2,3-*d*]pyrimidine antifolates with a thienoyl side chain (compounds **1**−**3**, respectively) were synthesized for comparison with compound **4**, the previous lead compound of this series. Conversion of hydroxyl acetylenthiophene carboxylic esters to thiophenyl-α-bromomethylketones and condensation with 2,4-diamino-6-hydroxypyrimidine afforded the 6-substituted pyrrolo[2,3-*d*]pyrimidine compounds of type **18** and **19**. Coupling with L-glutamate diethyl ester, followed by saponification, afforded **1**−**3**. Compound **3** selectively inhibited the proliferation of cells expressing folate receptors (FRs) α or β, or the proton-coupled folate transporter (PCFT), including KB and IGROV1 human tumor cells, much more potently than **4**. Compound **3** was more inhibitory than **4** toward β-glycinamide ribonucleotide formyltransferase (GARFTase). Both **3** and **4** depleted cellular ATP pools. In SCID mice with IGROV1 tumors, **3** was more efficacious than **4**. Collectively, our results show potent antitumor activity for **3** in vitro and in vivo, associated with its selective membrane transport by FRs and PCFT over RFC and inhibition of GARFTase, clearly establishing the 3-atom bridge as superior to the 1-, 2-, and 4-atom bridge lengths for the activity of this series.

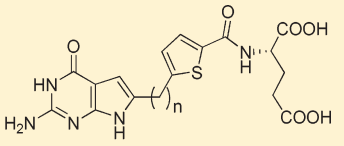

1 n = 1
2 n = 2
3 n = 3

INTRODUCTION

In the era of targeted therapeutics for cancer, antifolates continue to occupy a unique niche in the treatment of a variety of malignancies including acute lymphoblastic leukemia, lymphomas, osteosarcoma, and malignant pleural mesothelioma.[1] Clinically relevant antifolates (Figure 1) such as methotrexate (MTX), pemetrexed (PMX), and raltitrexed (RTX) are all substrates for the ubiquitously expressed reduced folate carrier (RFC), which is the major folate transport system in tissues and tumors.[2] RFC levels and activities are important determinants of drug efficacy, and loss of RFC is a common mode of antifolate drug resistance.[2,3] However, RFC is also expressed in normal tissues such that it is likely to be a determinant of dose-limiting drug toxicity, although other factors such as systemic folate levels (both circulating and intracellular forms), capacities to synthesize antifolyl polyglutamates, and rates of cell proliferation all come into play.[2]

Along with RFC, other folate membrane transporters are recognized as important for physiologic functions in relation to

Received: June 8, 2011
Published: August 31, 2011

dx.doi.org/10.1021/jm200739e | *J. Med. Chem.* 2011, 54, 7150–7164

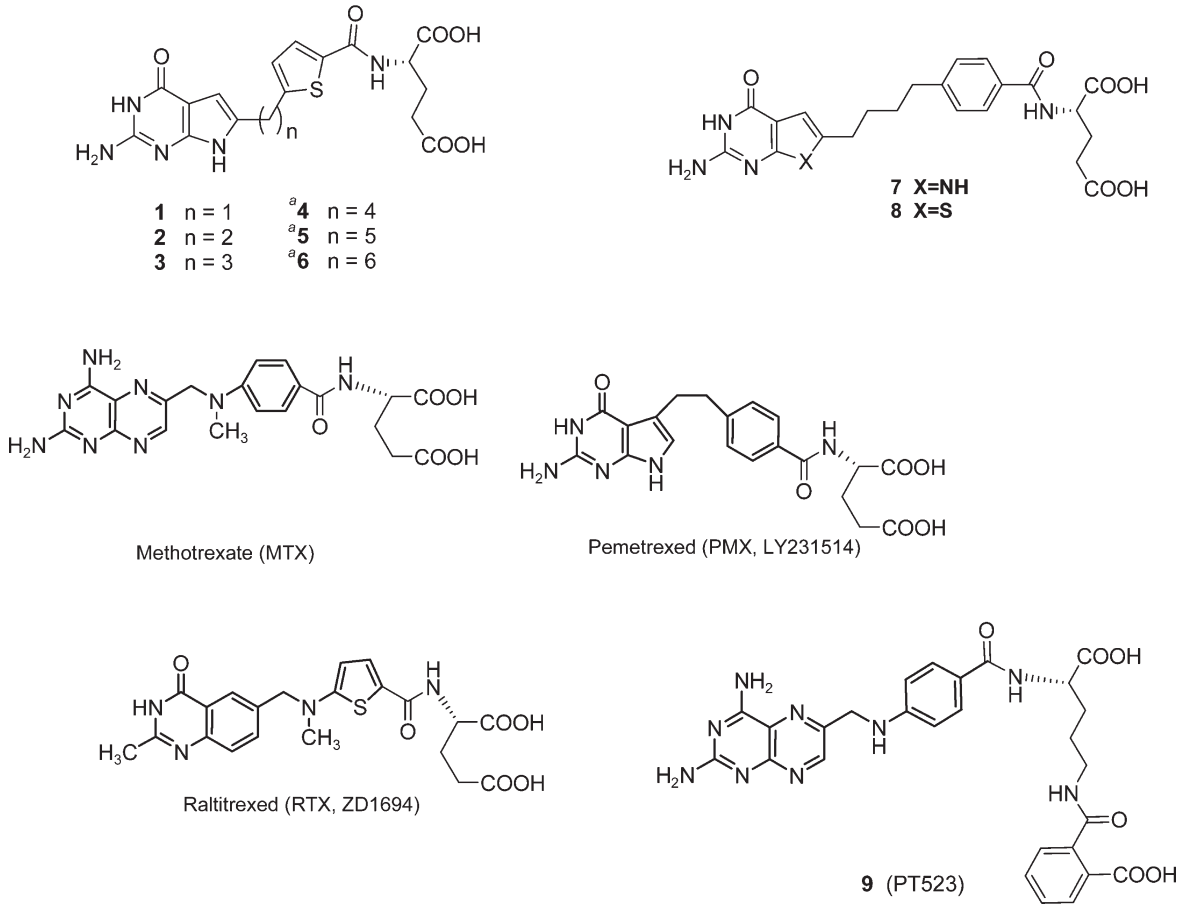

Figure 1. Structures for classical antifolates and novel pyrrolo- and thieno[2,3-*d*]pyrimidine antifolates. Compounds **4**−**8** were previously described.[12−14] MTX is a dihydrofolate reductase inhibitor, whereas PMX and RTX are primarily thymidylate synthase inhibitors. Compound **9** is a novel antifolate and dihydrofolate reductase inhibitor[16] that is an active and highly selective substrate for RFC over PCFT.[6,15]

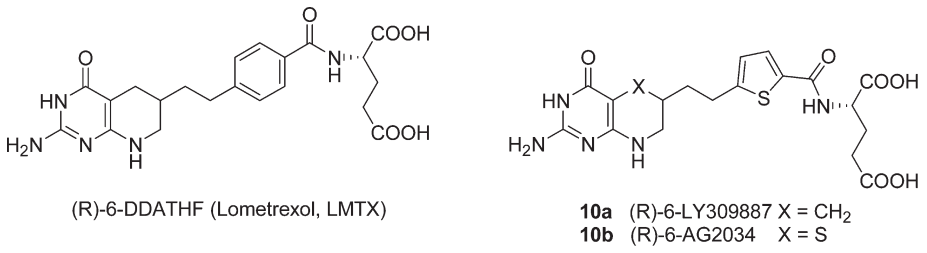

Figure 2. Structures for previous generation GARFTase inhibitors. Lometrexol was originally synthesized by Taylor et al.[17] and was the first antifolate inhibitor of GARFTase.[18,19] Compounds **10a** and **10b** are second generation GARFTase inhibitors as described in the text.[20−22].

in vivo folate homeostasis and likely contribute to assorted clinical manifestations of folate deficiency. For instance, folate receptor (FR) α is expressed in epithelial tissues such as the renal tubules and cerebral microvasculature where it is important in folate reabsorption and folate transport across the blood−brain barrier, respectively.[4] A folate-proton symporter, the proton−coupled folate transporter (PCFT), is expressed in the upper small intestine (e.g., jejunum) where it represents the primary mode of dietary folate absorption, and its loss is causal in the autosomal recessive folate-deficient condition termed hereditary folate malabsorption.[5−7]

Interestingly, these non-RFC transport mechanisms have also attracted attention for their potentials in chemotherapy drug targeting, particularly for cancer, since FRs are expressed in a subset of malignancies such as ovarian and endometrial cancers,[4,8] and PCFT is present at high levels in assorted solid tumors (including lung cancers, ovarian cancer, and hepatomas).[6,9] Further, PCFT is maximally active at pHs approximating those attained in the solid tumor microenvironment.[6,7,10] Examples of folate-based therapeutics for cancer with selective transport by FRs include a folate-conjugated microtubule inhibitor licensed by Bristol-Myers Squibb (http://www.cancer.gov/drugdictionary/ ?CdrID=575735), and *N*-[(4-{(6*RS*)-2-hydroxymethyl-4-oxo-4,6,7,8-tetrahydro-3*H*-cyclopenta[*g*]quinazolin-6-yl](prop-2-yn-1-yl)amino}phenyl)-carbonyl]-L-(-glutamyl-D-glutamic acid (ONX0801),[11] a small molecule antifolate licensed by Onyx Pharmaceuticals, which is

Scheme 1[a]

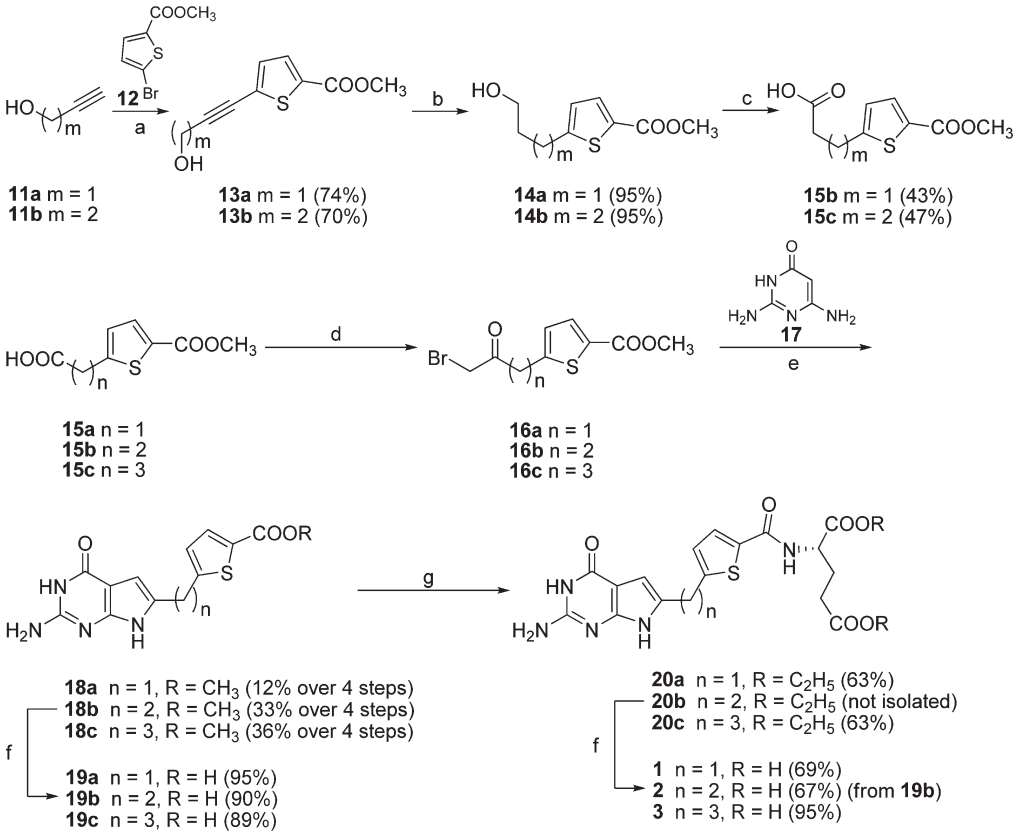

[a] Reagents and conditions: (a) CuI, $PdCl_2$, PPh_3, Et_3N, CH_3CN, microwave, 100 °C, 10 min; (b) 10% Pd/C, H_2, 55 psi, MeOH, 4 h; (c) H_2SO_4, CrO_3, 0 °C∼RT; (d) i. oxalyl chloride, CH_2Cl_2, reflux, 1 h; ii. diazomethane, Et_2O, RT, 1 h; iii. HBr, 70−80 °C, 2 h; (e) DMF, RT, 3 days; (f) i. 1 N NaOH, RT, 12 h; ii. 1 N HCl; (g) *N*-methylmorpholine, 2-chloro-4,6-dimethoxy-1,3,5-triazine, L-glutamate diethyl ester hydrochloride, DMF, RT, 12 h.

a potent inhibitor of thymidylate synthase. Both of these compounds are in clinical trials.

We reported[9,12−15] the 6-substituted pyrrolo- and thieno[2,3-*d*]-pyrimidine benzoyl L-glutamate antifolate scaffolds **7** and **8** (Figure 1) to identify analogues with selective membrane transport by PCFT and/or FRs but not by RFC. For both series, the lengths of the bridge region were systematically tested. The most active agents had 3- or 4-carbon bridge lengths and were potent inhibitors of β-glycinamide ribonucleotide (GAR) formyltransferase (GARFTase), which catalyzes the third step in de novo purine biosynthesis in which GAR is converted to formyl GAR with 10-formyl tetrahydrofolate as the one-carbon donor. Drug potencies declined with increasing (>4 carbons) or decreasing (<3 carbons) bridge lengths and were further impacted by isosteric replacement of the benzoyl ring of the pyrrolo[2,3-*d*]pyrimidine series with a thienoyl ring (compounds **4**−**6**).[9,12−15] The 6-substituted pyrrolo[2,3-d]pyrimidine thienoyl antifolate with a 4-carbon bridge (compound **4** in Figure 1) was the most active analogue toward both FR- and PCFT-expressing tumors in vitro and in vivo.[14] However, analogues of this series with less than 4 carbons in the bridge region were not previously synthesized and tested.

A number of other antifolates have been previously reported to inhibit GARFTase as their principal cellular targets. Lometrexol [(6*R*)5,10-dideazatetrahydrofolate; LMTX] (Figure 2) originated from a collaboration between academic laboratories and the Eli Lilly Corporation in the mid 1980s and shortly thereafter was described as an inhibitor of de novo purine biosynthesis at GARFTase.[17−20] For second generation GARFTase inhibitors, replacement of the 1,4-phenyl ring by a 2,5-thienyl ring increased potency over LMTX (e.g., **10a** (LY309887)[20,21] and **10b** (AG2034)[22]). LMTX, **10a**, and **10b** were all entered into clinical trials;[21−24] the toxicities experienced were likely due, at least in part, to their transport by RFC and polyglutamylation by folypolyglutamate synthetase in susceptible normal tissues. These early studies provided further impetus to developing agents with FR and PCFT transport selectivity over RFC.

In this article, we describe the synthesis and biological properties of compounds **1**−**3**, analogues of compound **4** with 1 to 3 bridge carbons, respectively, linking a 6-substituted pyrrolo[2,3-*d*]-pyrimidine moiety with a thienoyl ring, for direct comparison with compound **4**. Our results demonstrate the dramatically increased potency of compound **3** toward both PCFT- and FR-expressing cells, associated with its greater inhibition of intracellular GARFTase. In an efficacy trial toward severe combined immunodeficient (SCID) mice bearing early stage IGROV1 ovarian carcinoma, compound **3** was substantially more active than compound **4**.

CHEMISTRY

The synthesis of target compounds **1**−**3** is shown in Scheme 1. A palladium-catalyzed Sonogashira coupling of 5-bromo-thiophene-2-

dx.doi.org/10.1021/jm200739e |*J. Med. Chem.* 2011, 54, 7150–7164

Table 1. IC_{50}s (in nM) for 6-Substituted Pyrrolo[2,3-*d*]pyrimidine Thienoyl Antifolates 1−4 and Classical Antifolates in hRFC-, hPCFT-, and FR-Expressing Cell Lines[a]

	hRFC		FRα		FRβ		hPCFT		hRFC/FRα/hPCFT		hRFC/FRα/hPCFT	
antifolate	PC43-10	R2	RT16	RT16 (+ FA)	D4	D4 (+ FA)	R2/hPCFT4	R2(VC)	KB	KB (+ FA)	IGROV1	IGROV1 (+ FA)
1	>1000	>1000	122 (86)	>1000	ND	ND	291 (71)	>1000	41.9 (24)	>1000	>1000	>1000
2	>1000	>1000	38.9 (10.2)	>1000	6.58 (0.95)	>1000	135 (18)	>1000	3.22 (0.50)	>1000	122.7 (32.2)	>1000
3	101.0 (16.6)	273.5 (49.1)	0.31 (0.14)	>1000	0.17 (0.03)	>1000	3.34 (0.26)	288 (12)	0.26 (0.03)	>1000	0.55 (0.10)	>1000
4	>1000	>1000	1.82(0.28)	>1000	0.57(0.09)	>1000	43.4(4.1)	>1000	0.55(0.10)	>1000	0.97(0.12)	>1000
MTX	12(1.1)	216(8.7)	114(31)	461(62)	106(11)	211(43)	121 (17)	>1000	6.0(0.6)	20(2.4)	21(3.4)	22(2.1)
PMX	138(13)	894(93)	42(9)	388(68)	60(8)	254(78)	13.2(2.4)	974 (18)	68(12)	327(103)	102(25)	200(18)
RTX	6.3(1.3)	>1000	15(5)	>1000	22(10)	746(138)	99.5(11.4)	>1000	5.9(2.2)	22(5)	12.6(3.3)	20(4.3)
LMTX	12(2.3)	>1000	12(8)	>188(39)	2.6(1.0)	275(101)	38.0(5.3)	>1000	1.2(0.6)	31(7)	3.1(0.9)	16(6)
9	1.28(0.18)	>1000	409(51)	864(39)	ND	ND	>1000	>1000	5.26(1.07)	2.90(0.16)	3.47(0.48)	2.47(0.38)

[a] Growth inhibition assays were performed for CHO sublines engineered to express hRFC (PC43-10), FRs (RT16, D4), or hPCFT (R2/hPCFT4) for comparison with transporter-null [R2, R2(VC)] CHO cells and for the KB and IGROV1 tumor sublines (expressing hRFC, FRα, and hPCFT), as described in the Experimental Procedures section. For the FR experiments, growth inhibition assays were performed in the presence and the absence of 200 nM folic acid (FA). The data shown are mean values from 2−10 experiments (±SEM in parentheses). Results are presented as IC_{50} values (in units of nM), corresponding to the concentrations that inhibit growth by 50% relative to cells incubated without the drug. Data for **4**, MTX, PMX, RTX, LMTX, and **9** were previously published.[12−15] ND: not determined.

carboxylic acid methyl ester, **12**, with prop-2-yn-1-ol, **11a**, or but-3-yn-1-ol, **11b**, afforded unsaturated alcohols **13a** and **13b**, respectively, which were catalytically hydrogenated to give the saturated alcohols **14a** and **14b** in quantitative yield. Subsequent oxidation of **14a** and **14b** using Jones reagent afforded the carboxylic acids **15b** and **15c**. Compound **15a** is commercially available. The carboxylic acids **15a−c** were then converted to the acid chlorides and immediately reacted with diazomethane followed by 48% HBr to give the desired α-bromomethylketones **16a−c**. Condensation of 2,6-diamino-3*H*-pyrimidin-4-one, **17**, with **16a−c** at room temperature for 3 days afforded the 2-amino-4-oxo-6-substituted-pyrrolo[2,3-*d*]pyrimidines **18a−c**. Hydrolysis of **18a−c** afforded the corresponding free acids **19a−c**. Subsequent coupling with the L-glutamate diethyl ester using 2-chloro-4,6-dimethoxy-1,3,5-triazine as the activating agent afforded the diesters **20a−c**. Final saponification of the diesters gave the desired compounds **1−3**.

BIOLOGICAL EVALUATION AND DISCUSSION

6-Substituted Pyrrolo[2,3-*d*]pyrimidine Thienoyl Antifolates As Potent Inhibitors of Tumor Cell Proliferation. Our previous studies of 6-substituted pyrrolo- and thieno[2,3-*d*]-pyrimidine benzoyl analogues showed that the intramolecular distance between the bicyclic scaffold and the L-glutamate was critical to inhibitory potencies and that an isosteric thienoyl-for-benzoyl substitution in the side chain conferred dramatically enhanced antiproliferative activities for analogues with 4 (compound **4**)- and 5 (compound **5**)-carbon bridge lengths (Figure 1) compared to the corresponding benzoyl analogues.[9,12−15] In the present study, we expanded the 6-substituted pyrrolo[2,3-*d*]pyrimidine thienoyl series of antifolates to include analogues with truncated bridge lengths of 1−3 carbons (compounds **1−3**) (Figure 1).

Compounds **1−3** were tested for their capacities to inhibit the proliferation of a series of isogenic Chinese hamster ovary (CHO) cell lines individually expressing each of the major human (anti)folate uptake systems including human RFC (hRFC) (PC43-10), FRα (RT16), FRβ (D4), and human PCFT (hPCFT) (R2/hPCFT4).[12,13,15] Additional drug screening was done with KB (nasopharyngeal) and IGROV1 (ovarian) human tumor cell lines that express RFC, PCFT, and FRα. For these experiments, cells were continuously exposed to a wide range of drug concentrations in standard RPMI1640/10% dialyzed fetal bovine serum (dFBS) (for PC43-10) or in folate-free RPMI/10% dFBS, supplemented with 2 nM (RT16, D4, KB, IGROV1) or 25 nM leucovorin [(6*R*,*S*)5-formyl tetrahydrofolate (LCV)] (R2/hPCFT4). Relative cell numbers were assessed after 96 h. Negative controls for RFC- and PCFT-expressing CHO sublines included the RFC-, FR-, and PCFT-null MTXRIIOua^{R}2-4 CHO parental cell line used for transfections (hereafter, designated R2) or vector control R2 cells [R2(VC)], both cultured under the same conditions. For FR-expressing cells, FR-mediated drug uptake was confirmed by treating a parallel culture with the antifolates, along with excess (200 nM) folic acid to block FRs. Results with compounds **1−3** were compared to those for compound **4** and for classical antifolates including MTX, PMX, LMTX, RTX, and compound **9** (Figures 1 and 2). These results are summarized in Table 1.

The known classical antifolates were all growth inhibitory toward the RFC-, PCFT-, and FR-expressing CHO sublines. Compound **3** was more active than the classic agents and likewise more so than compounds **1** and **2**, or compound **4**, the 4-carbon bridge analogue and the previous lead compound of this series.[14] This was most impressively reflected in the ~11-fold decrease in IC_{50} (~3 nM) toward PCFT-expressing R2/hPCFT4 cells and the ~6-fold decrease in IC_{50} toward FRα-expressing RT16 cells with **3** compared to **4**. Activity substantially declined for compounds **1** and **2** with 1- and 2-carbon bridge lengths, respectively. While **1** and **2** were inert toward RFC-expressing PC43-10 cells and RFC-, PCFT-, and FR-null R2 cells up to 1000 nM drug, compound **3** showed evidence of a non-FR, non-PCFT cellular uptake process at higher drug concentrations (seemingly in part mediated by RFC and also by a non-RFC uptake mechanism), although substantial FR- and PCFT-selectivity over RFC (as reflected in relative IC_{50}s) was nonetheless preserved (Table 1). Compounds **3** and **4** showed slightly (~2-fold) increased activities (decreased IC_{50}s) toward FRβ-expressing D4 cells over those for FRα-expressing RT16 cells, although this

was statistically significant (i.e., $p < 0.05$) only for compound **4**. For RT16 and D4 sublines with both compounds **3** and **4**, growth inhibition was abolished with excess (200 nM) folic acid. Analogous results were observed with KB and IGROV1 human tumor cells such that the IC_{50}s for compound **3** were an impressive 0.26 nM and 0.55 nM, respectively, or ~2-fold lower than the IC_{50}s for compound **4**.

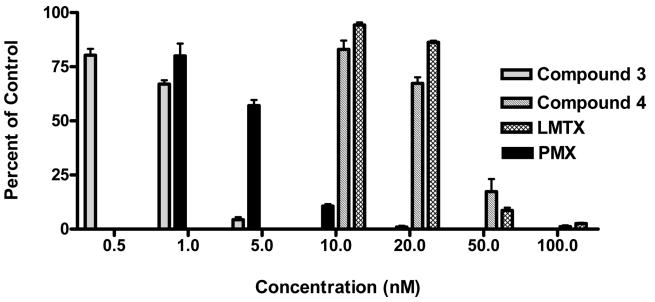

Figure 3. Colony formation assay. R2/hPCFT4 cells were inoculated into 60 mm dishes (200 cells per dish), in the presence or absence of a range of concentrations of compound **3**, compound **4**, LMTX, or PMX. Colonies were enumerated, and the results are presented as the percent of control treated identically but without drugs as mean values from 3 experiments (±SEM). IC_{50}s for **3**, **4**, PMX, and LMTX were 1.4 nM, 27.2 nM, 4.9 nM, and 29.7 nM, respectively.

The results of the cell proliferation assays for R2/hPCFT4 cells were recapitulated in the results of colony-forming assays over 10 days in the continuous presence of **3** (0.5−10 nM), **4** (10−100 nM), PMX (1−20 nM), or LMTX (10−100 nM) (Figure 3). IC_{50}s in colony-forming assays closely approximated those in the cell proliferation assays (Table 1) with R2/hPCFT4 cells and were 1.4 nM, 27.2 nM, 4.94 nM, and 29.7 nM, respectively. Collectively, these results establish significantly higher potencies for compound **3** over **4** as an inhibitor of proliferation for cells expressing FRs and/or PCFT with substantial selectivity for transport by FRs and PCFT over RFC.

Membrane Transport Characteristics for Compound 3. Compound **3** showed demonstrably higher antiproliferative activities toward FR- and hPCFT-expressing cells (Table 1) compared to compound **4** and the classical antifolate drugs, whereas hRFC-directed activity was substantially decreased (compound **3**) or was altogether undetectable up to 1000 nM drug (compounds **1**, **2**, and **4**). To further examine biochemical measures of drug transport by hRFC, FR, and hPCFT, functional assays were performed for compounds **2**, **3**, and **4**, the most active compounds of the series.

As competitive inhibitors of transport of [^{3}H]MTX (0.5 μM) by hRFC in PC43-10 cells (2 min influx, 37 °C), compounds **2**−**4** (at 10 μM) were all poorly inhibitory, with **3** showing the greatest effect (~20% inhibition relative to control) (Figure 4, panel A). The inhibitory effects of compounds **2**−**4** toward hRFC were substantially less than the inhibitions detected with

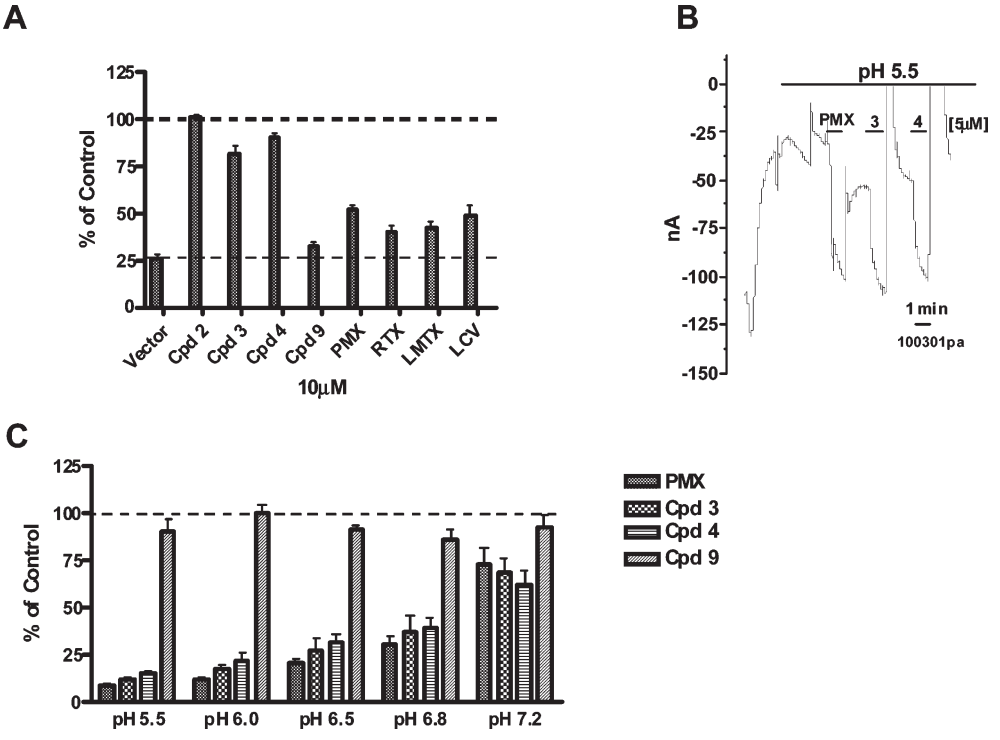

Figure 4. Transport assays for RFC and PCFT cellular uptake. Panel A: PC43-10 cells ectopically expressing hRFC but no FRs or hPCFT were assayed for [^{3}H]MTX (0.5 μM) uptake at pH 7.2 in the presence of compounds **2**−**4** or the established RFC substrates, **9**, PMX, RTX, LMTX, or LCV (each at 10 μM). Results are compared to those for transporter-null R2 (VC) cells (labeled "vector"). Panel B: substrate-induced currents (nA) were recorded in individual *Xenopus* oocytes injected with wild type hPCFT cRNA and voltage clamped to a holding potential of −90 mV. Oocytes were perfused with ND90 solution at pH 5.5 with PMX, compound **3**, or compound **4** (all at 5 μM). The design of these experiments was identical to those previously reported.[15,25] Panel C: R2/hPCFT4 cells, ectopically expressing hPCFT, were assayed for cellular uptake of [^{3}H]MTX (0.5 μM) from pH 5.5 to pH 7.2 in the presence of PMX, **3**, **4**, or **9** (each at 10 μM). For panels A and C, the results are expressed as the percent of control (absence of inhibitors) and as mean values ±SEM from 3 experiments. Details for all the transport and binding assays are in the Experimental Procedures section.

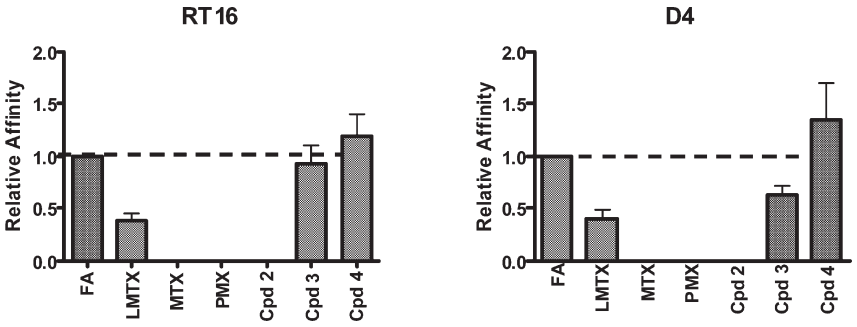

Figure 5. FRα and FRβ binding assays for assorted antifolates. Data are shown for the effects of the unlabeled ligands with FRα-expressing RT16 CHO cells and FRβ-expressing D4 CHO cells. Relative binding affinities for assorted folate/antifolate substrates were calculated as the inverse molar ratios of unlabeled ligands required to inhibit [^{3}H]folic acid binding by 50%. By definition, the relative affinity of folic acid (FA) is 1. Results are presented as mean values ±SEM from 3 experiments. Experimental details are provided in the Experimental Procedures section.

Table 2. Kinetic Constants for hPCFT[a]

substrate	parameter	pH 5.5	pH 6.8
MTX[b]	K_t (μM)	0.28 ± 0.02	4.52 ± 0.19
MTX[b]	V_{max} (pmol/mg/min)	31.23 ± 4.31	13.72 ± 2.26
PMX[b]	K_i (μM)	0.096 ± 0.012	1.54 ± 0.17
3	K_i (μM)	0.13 ± 0.01	1.82 ± 0.07
4[b]	K_i (μM)	0.13 ± 0.01	1.95 ± 0.02

[a] Kinetic constants for MTX (K_t and V_{max}) were determined with [^{3}H]MTX by Lineweaver−Burke plots with R2/hPCFT4 cells, whereas K_i values were determined by Dixon plots with [^{3}H]MTX as the substrate and a range of inhibitor concentrations in R2/hPCFT4 cells. Results are presented as mean values ± standard errors from 3 experiments. [b] From Wang et al. (ref 14).

10 μM of **9**, PMX, RTX, LMTX, or LCV, all established hRFC substrates.

With FRs and the most active analogues (compounds **2**−**4**), we used competitive binding assays to measure the abilities of unlabeled ligands to compete for FR binding with [^{3}H]folic acid. For these assays, RT16 (FRα) and D4 (FRβ) cells were briefly treated with acid-buffered saline to dissociate FR-bound folate, then with [^{3}H]folic acid (at neutral pH) in the presence of unlabeled competitors including compounds **2**, **3**, and **4**, classic antifolates (LMTX, PMX, and MTX), or unlabeled folic acid (50 nM). Cells were washed (neutral pH) after which FR-bound [^{3}H]folic acid was measured with results expressed as picomole of [^{3}H]folic acid per milligram of cellular protein. Relative inhibitor affinities were calculated as the inverse molar ratios of the concentrations of unlabeled (anti)folates required to decrease bound [^{3}H]folic acid by 50%. By this assay, binding of **2** was undetectable and analogous to that for MTX and PMX, both poor substrates for FRs in spite of detectable low levels of growth inhibition toward FR-expressing cells. There was no relationship between binding affinities for FRα or FRβ (Figure 5) and inhibition of proliferation of RT16 or D4 CHO cells, respectively, by compounds **3** and **4** (Table 1).

To confirm membrane transport of compound **3** by PCFT, we used electrophysiology experiments with *Xenopus* oocytes microinjected with hPCFT cRNA and clamped at −90 mV using a bath of pH 5.5. As for established PCFT substrates (e.g., PMX),[15,16] compounds **3** and **4** at 5 μM induced currents, whereas current (Figure 4, panel B) was not induced in oocytes microinjected with H_2O in lieu of hPCFT cRNA (not shown). There was no obvious difference in the current induced by compound **3** and that by compound **4** or PMX.

As an additional measure of transport by hPCFT, we compared compound **3** to **4** and to PMX or **9** (at 10 μM) as competitors of hPCFT-mediated transport of [^{3}H]MTX (0.5 μM) in R2/hPCFT4 cells from pH 5.5 to pH 7.2. Whereas **9** did not inhibit [^{3}H]MTX transport by hPCFT at any pH, compounds **3**, **4**, and PMX were all potent and essentially equivalent inhibitors, with the relative extents of inhibition dramatically increasing from pH 6.8 to pH 5.5 (Figure 4, panel C).

To calculate K_i values as measures of relative binding affinities for hPCFT, we performed Dixon analyses at pH 5.5 and pH 6.8 with [^{3}H]MTX and variable concentrations of unlabeled substrates, including compounds **3**, **4**, and PMX. By this analysis, K_is for compounds **3** and **4** were nearly identical at pHs 5.5 and 6.8, and only slightly higher (~35% and 18%, respectively) than the K_is for PMX at pH 5.5 and pH 6.8 (Table 2).

Collectively, these results demonstrate that transport characteristics for compounds **3** and **4** for FRs and hPCFT are nominally different, and for hPCFT only slightly different from those for PMX. However, unlike PMX, transport of **3** and **4** by hRFC appears to be minimal. Clearly, transport differences between **3** and **4** do not account for the substantial differences in inhibitions of cell proliferation or colony formation.

Identification of GARFTase As the Primary Intracellular Target for Compound 3. The dramatic increase in growth inhibitory potency of compound **3** over **4** or PMX toward hPCFT- or FR-expressing cell lines including KB and IGROV1 human tumor cells does not appear to reflect differences in FR or hPCFT transport parameters for these drugs. We previously reported that compound **4** was a potent inhibitor of GARFTase, the third step in the de novo purine nucleotide biosynthetic pathway, and that reduced cell proliferation was directly attributed to GARFTase inhibition in cultured cells.[14] To identify the targeted pathway for compound **3** (de novo purine nucleotide versus thymidylate biosynthesis), we tested exogenous nucleosides for their capacities to circumvent growth inhibition by this analogue toward R2/hPCFT4 cells. Results were compared to those for PMX, reported to act as an inhibitor of both purine nucleotide (primarily at 5-amino-4-imidazolecarboxamide ribonucleotide (AICAR) formyltransferase (AICARFTase) and less so at GARFTase) and thymidylate synthase,[26,27] and of LMTX, an established inhibitor of GARFTase.[18−20]

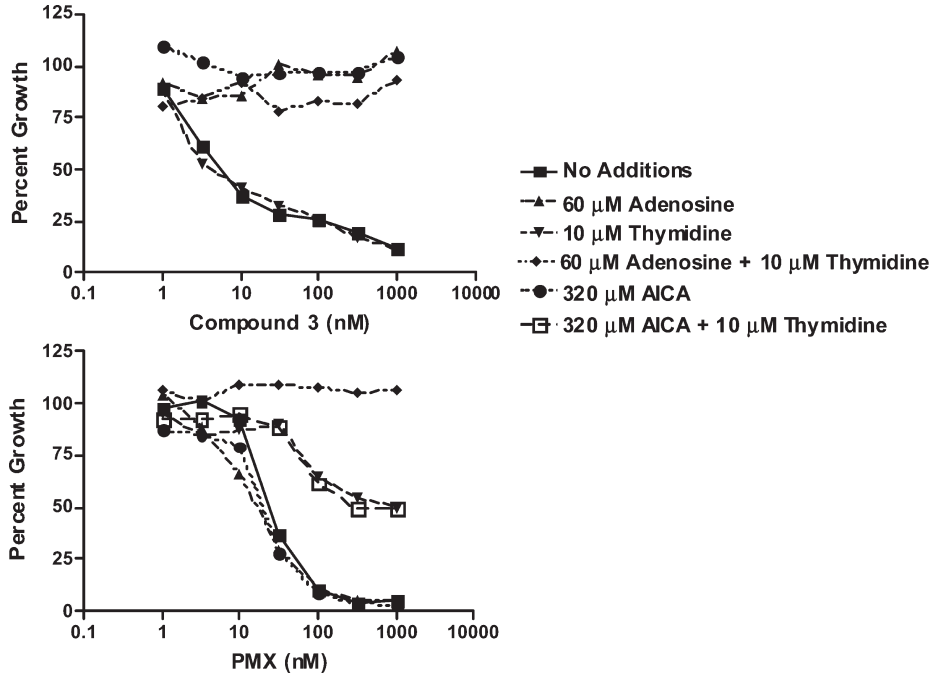

Figure 6. Protection of R2/hPCFT4 cells from growth inhibition by the 6-substituted pyrrolo[2,3-*d*]pyrimidine thienoyl antifolate **3** (upper) and PMX (lower) in the presence of nucleosides and 5-amino-4-imidazolecarboxamide (AICA). Proliferation inhibition was measured for R2/hPCFT4 cells over a range of concentrations of compound **3**, in the presence or absence of adenosine (60 μM), thymidine (10 μM), and/or AICA (320 μM), as described in the Experimental Procedures section. Results were normalized to cell density in the absence of the drug. Results shown are representative data from experiments performed in triplicate.

Whereas thymidine (10 μM) also protected R2/hPCFT4 cells from the growth inhibitory effects of low concentrations (<50 nM) of PMX, at higher PMX concentrations, protection was incomplete with thymidine either in the presence or absence of 5-amino-4-imidazolecarboxamide (AICA) (320 μM) (Figure 6, lower panel), which is metabolized to AICAR (circumvents drug effects at GARFTase). Adenosine (60 μM) could not circumvent effects of PMX. However, growth inhibition by PMX was completely reversed by adenosine combined with thymidine. Analogous results were previously described for nucleoside protection from the inhibitory effects of PMX for CCRF-CEM cells.[27] In contrast, for both LMTX (results not shown) and compound **3** (Figure 6, upper panel), growth inhibition was abolished by either adenosine or AICA alone. These results establish de novo purine nucleotide biosynthesis as the targeted pathway for compound **3** and GARFTase as the principal intracellular enzyme target, analogous to compound **4**[14] and LMTX.[18]

To confirm the inhibition of purine nucleotide biosynthesis by compounds **3** and **4**, we measured ATP pools by HPLC in R2/hPCFT4 cells treated with 1 μM of these antifolates for 24 h at pH 6.8. Results were compared to those of PMX and LMTX (both at 1 μM) (Figure 7A). Whereas PMX treatment only minimally impacted ATP pools (~17%), for both **3** and **4**, ATP pools were profoundly depleted (~90%) and exceeded the decrease resulting from treatment with LMTX (~76%).

To directly measure GARFTase activity in R2/hPCFT4 cells by growth inhibitory antifolates (**3**, **4**, PMX, and LMTX), we used an in situ GARFTase activity assay which measures the incorporation of [^{14}C]glycine into [^{14}C]formyl GAR in the presence of azaserine.[12,18] For these experiments, the protocol was modified[15] such that the medium was at pH ~6.9 during 15 h of antifolate treatment, after which cells were washed and resuspended in fresh medium (pH ~7.2) with azaserine, L-glutamine, and [^{14}C]glycine for an additional 8 h. Cells were treated with trichloroacetic acid; the acid soluble metabolites were ether-extracted and fractionated by anion exchange chromatography so that [^{14}C]formyl GAR could be quantitated.

The results showed that in R2/hPCFT4 cells for which PCFT is the only mode of transport, GARFTase was inhibited in the order **3** > **4** > PMX > LMTX (Figure 7B). For compounds **3** and **4**, IC_{50}s for in situ inhibition of GARFTase were 0.69 nM and 1.96 nM, respectively. Thus, the IC_{50}s for GARFTase inhibition in R2/PCFT4 cells generally parallel those for the inhibition of cell proliferation (Table 1). However, the IC_{50}s for GARFTase inhibition were substantially lower.

These results establish that compound **3** is a potent inhibitor of GARFTase *in cells* and that the increased antiproliferative effects of **3** over **4** are likely due primarily to its increased inhibition of intracellular GARFTase rather than to differences in membrane transport. For both compounds **3** and **4**, GARFTase inhibition results in a profound inhibition of de novo purine nucleotide biosynthesis, as reflected in a dramatic decrease in total cellular ATP pools exceeding that for LMTX. The failure of PMX to significantly deplete ATP pools reflects its poor inhibition of GARFTase, as previously reported.[27]

In Vivo Antitumor Efficacy with Compound 3. An in vivo drug efficacy trial was designed with 10 week old female ICR SCID mice (Taconic) implanted with subcutaneous human IGROV1 ovarian tumors, which express hRFC, hPCFT, and FRα. Mice were maintained ad libitum on a folate-deficient diet in order to decrease levels of serum folates (~5-fold) to concentrations approximating those reported in humans on a folate-fortified diet.[14] Mice maintained on a standard

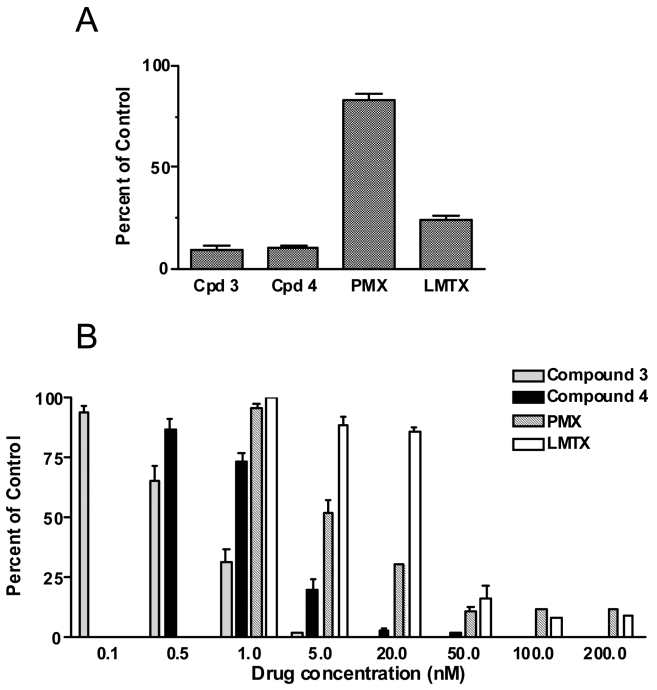

Figure 7. Intracellular ATP levels and in situ GARFTase inhibition in R2/hPCFT4 cells treated with compound **3**, compound **4**, LMTX, and PMX. Panel A: R2/hPCFT4 cells were treated with 1 μM **3**, **4**, PMX, or LMTX, or solvent (0.5% DMSO for **3** and **4**, H_2O for PMX and LMTX) for 24 h. Cells were washed, and nucleotides were extracted and analyzed by HPLC. Results are shown for percentage control ATP after the drug treatments. Panel B: GARFTase activity and inhibition were evaluated in situ with R2/hPCFT4 cells. Accumulation of [^{14}C]formyl GAR from [^{14}C]glycine was measured in R2/hPCFT4 cells treated with the antifolates. The production of [^{14}C]formyl GAR was calculated as a percent of vehicle control over a range of antifolate concentrations. Results are presented as the mean values ± standard errors from 3 experiments. Methodologic details are described in the Experimental Procedures section. Results with PMX and LMTX were from Kugel Desmoulin et al.[15] IC_{50}s were as follows: 0.69 nM, **3**; 1.96 nM, **4**; 31.5 nM LMTX; and 7.3 nM, PMX.

folate-replete diet were included as controls. Mice were pooled and implanted subcutaneously with IGROV1 tumor fragments, then nonselectively randomized into control and treatment groups. A Q4dx5 schedule was used with intravenous administration of compounds **3** (40 and 25 mg/kg/injection) and **4** (180 mg/kg/injection and 112.5 mg/kg/injection) on days 3, 7, 11, 15, and 19 postimplantation. Mice were observed and weighed daily; tumors were measured twice per week. Figure 8 shows results for compound **4** at both 112.5 and 180 mg/kg/injection and for compound **3** at 40 mg/kg/injection. Complete results for the in vivo experiment shown in Figure 8 are summarized in Table 1S in the Supporting Information.

For mice maintained on the folate-deficient diet, antitumor activities for compound **3** (40 and 25 mg/kg/injection) were striking with T/C values of 14% and 16%, and gross log kill values of 2.7 and 3.3, respectively. The treatment regimen with compound **3** was very well tolerated, and the only adverse dose-limiting symptom observed was reversible body weight loss. Recovery was excellent with good host recovery time (≤10 days) when maintained on a folate-deficient diet. Weight loss ranged from 6.3% (25 mg/kg/inj; nadir day 13; full recovery day 27 or 8 days post-last treatment) to 9.4% (40 mg/kg/inj; nadir day 21; full recovery 10 days post-last treatment). By comparison, compound **4** (180 mg/kg/inj) gave a 32% T/C and 2.3 gross log kill against the IGROV1 tumor model with one lethality, resulting from GI epithelial damage (based on necropsy). At 112.5 mg/kg/injection, compound **4** produced a 44% T/C with no lethalities. For compound **4** at 180 mg/kg/injection, a weight loss nadir of 8.8% was reached on day 21 with 99% recovery by day 31.

Whereas antitumor activity for **4** was completely ablated in mice maintained on the standard folate replete diet, for compound **3** with a standard diet, a T/C of 67% and gross log kill of 0.8 were measured with minimal toxicity (2.7−5% reversible body weight loss). The latter was sufficient to be considered as minimally active (by log kill standards), even in the presence of substantially elevated serum folate.

The results of the in vivo efficacy trial with the IGROV1 tumor demonstrate potent antitumor activities with compound **3**, exceeding that for compound **4** and reflecting cellular uptake by FRα and hPCFT over hRFC, and potent inhibition of intracellular GARFTase.

CONCLUSIONS

In this article, we expanded upon our previous report on a series of 2-amino-4-oxo-6-substituted-pyrrolo[2,3-*d*]pyrimidines with a side chain thienoyl ring with 4−6 bridge carbons as selective transport substrates for FRs and PCFT over RFC.[14] We systemically examined the effects of analogues with 1−3 bridge carbons compared to compound **4**, the 4-carbon bridge analogue and the previous lead compound for this series,[14] on proliferation of CHO cells with individual expressions of FRs, hPCFT, or hRFC, and on IGROV1 and KB human tumor cells expressing all three transport systems, in order to assess the effects of systematically varying the distance between the bicyclic scaffold and the L-glutamate moiety.

Our results establish that the 3-carbon bridge analogue, compound **3**, is substantially more active in vitro toward CHO cells that exclusively express FRs and/or hPCFT (~6- and 11-fold, respectively) than **4**, characterized by a 4-carbon bridge. For FR-expressing CHO cells, **1** (one carbon bridge) showed low level activity (394-fold less than compound **3** with FRα-expressing RT16 cells), and **3** was 38 (FRβ)- and 125-fold (FRα) more active than **2** (2-carbon bridge). Against hPCFT-expressing (R2/hPCFT4) cells, **3** was 40- and 87-fold more potent than **2** and **1**, respectively. Thus, increasing the bridge lengths from 1- to 3-carbon atoms sequentially increases potencies toward both FR- and hPCFT-expressing cells, and potencies further decrease with increasing chain length to 4 carbons. Accordingly, the 3-atom carbon bridge appears to be optimal for this series. Analogous results with compounds **1**−**4** were obtained in vitro with human KB and IGROV1 tumors with activity in the order of **3** > **4** ≫ **2** > **1**.

Interestingly, between **3** and **4**, there were no significant differences in transport properties for FRs or hPCFT that could explain differences in their antiproliferative effects. While low level RFC and/or non-RFC uptake components were implied for compound **3**, these would occur only at *substantially higher drug concentrations* than those that targeted FR- and hPCFT-expressing cells and would thus be unlikely to appreciably contribute to the inhibitory effects of this compound on cell proliferation or clonogenicity. Differences in inhibitory potencies between **3** and **4** toward *intracellular* GARFTase predominated. Although we

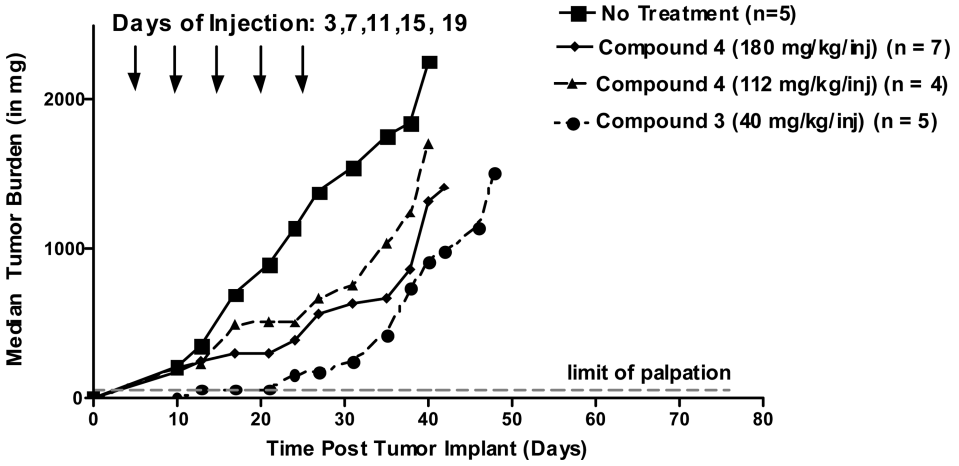

Figure 8. In vivo efficacy trial with compounds **3** and **4** with IGROV1 xenografts. Human IGROV1 tumors were implanted bilaterally into female ICR SCID mice maintained on a folate-deficient diet, and mice were nonselectively randomized into 4−7 mice/group. Compounds **3** (40 mg/mg) and **4** (180 mg/kg and 112.5 mg/kg), dissolved in 5% ethanol (v/v), 1% Tween-80 (v/v), and 0.5% $NaHCO_3$, were administered on a Q4dx5 schedule intravenously (0.2 mL/injection) on days 3, 7, 11, 15, and 19. Mice were observed and weighed daily; tumors were measured twice per week. For the experiment shown, antitumor activity was significant for compound **3** (14% T/C, 2.7 gross log kill) and exceeded that for compound **4** at either dose (32% and 44% T/C, 2.3 and 1.2 gross log kill, respectively, at 180 mg/kg and 112.5 mg/kg). The results are summarized in Table 1S in the Supporting Information.

were not able to detect differences in inhibitory potencies of monoglutamyl **3** and **4** toward isolated recombinant murine GARFTase (data not shown), the relevance of these findings to the intracellular mileau where antifolyl polyglutamates predominate[3] and are likely far more potent inhibitors of intracellular GARFTase[19] is uncertain. Against intracellular GARFTase, both **3** and **4** were inhibitory at concentrations substantially less than those required for the inhibition of cell proliferation or clonogenicity, suggesting that sustained inhibition of GARFTase and de novo purine biosynthesis are essential for cell killing in this CHO cell line model.[15] GARFTase inhibition was accompanied by substantial suppression of de novo purine nucleotide biosynthesis, as reflected in the depletion of cellular ATP pools.

We extended our promising in vitro findings with compound **3** in vivo using a challenging tumor model (IGROV1) with substantially lower levels of FRα than those in the KB tumor previously reported for **4**.[14] With subcutaneous IGROV1 tumors in SCID mice, compound **3** was more efficacious than compound **4**, as reflected in T/C and gross log kill and at much lower doses. Further, at the highest drug dose (180 mg/kg), compound **4** was lethal, resulting in the death of 1 of 7 mice in this trial. Clearly, compound **3** would permit a greater margin of safety than compound **4**, as less than maximum tolerated dosing can be administered with reduced toxicity accompanying substantially increased antitumor activity. This property would also be beneficial with potentially additive or synergistic drug combination regimens. Interestingly, compound **3** also preserved some level of activity even in the presence of elevated serum folate, unlike **4**, which was inactive under these conditions.

Collectively, our results establish that the pyrrolo[2,3-*d*]-pyrimidine thienoyl scaffold is particularly amenable to selective FR and PCFT transport compared to that of RFC and to potent GARFTase inhibition. Antiproliferative activity is substantially increased for this series with compound **3**, characterized by a 3-carbon bridge and a reduced intramolecular distance between the bicyclic scaffold and the L-glutamate compared to that of compound **4**. Our in vitro data for compounds **3** and **4** strongly imply that their relative inhibitory potencies toward intracellular GARFTase are the major determinants of relative drug activities for this series of analogues, likely secondary to their metabolism to polyglutamates. While it cannot be established with complete certainty from the available data that in vivo tumor selectivity for the active analogues derives from their selective cellular uptake by FRα and PCFT over RFC in tumors versus normal tissues, on the basis of our in vitro results, this is not unreasonable.

Although early preclinical studies with LMTX showed its substantial efficacy against a number of transplanted tumors accompanying its membrane transport by all the major systems including RFC, PCFT, and FRs,[20] when administered to patients in phase I, toxicity was not insignificant.[23] This is likely due at least in part to its excellent RFC substrate activity and its polyglutamylation in susceptible normal tissues. A similar explanation may account for the toxicity encountered with the second generation GARFTase inhibitors (**10a** and **10b**) in patients.[21,22,24]

On the basis of this promising lead analogue, future studies with compound **3** will further examine major biochemical determinants of its in vitro and in vivo activities, including its membrane transport properties and its metabolism to polyglutamates. Additional studies will expand in vivo testing to include a broader cohort of clinically relevant human tumor models expressing FRs and PCFT, including late stage tumors. These results will be included in future reports.

EXPERIMENTAL PROCEDURES

All evaporations were carried out in vacuum with a rotary evaporator. Analytical samples were dried in vacuo (0.2 mmHg) in a CHEM-DRY drying apparatus over P_2O_5 at 60 °C. Melting points were determined on a MEL-TEMP II melting point apparatus with a FLUKE 51 K/J electronic thermometer and are uncorrected. Nuclear magnetic resonance spectra for protons (^{1}H NMR) were recorded on a Bruker Avance II 400 (400 MHz) and 500 (500 MHz) spectrometer. The chemical shift values are expressed in ppm (parts per million) relative to

tetramethylsilane as an internal standard: s, singlet; d, doublet; t, triplet; q, quartet; m, multiplet; br, broad singlet. Thin-layer chromatography (TLC) was performed on Whatman Sil G/UV254 silica gel plates with a fluorescent indicator, and the spots were visualized under 254 and 366 nm illumination. Proportions of solvents used for TLC are by volume. Column chromatography was performed on a 230−400 mesh silica gel (Fisher, Somerville, NJ) column. The amount (weight) of silica gel for column chromatography was in the range of 50−100 times the amount (weight) of the crude compounds being separated. Columns were dry-packed unless specified otherwise. Elemental analyses were performed by Atlantic Microlab, Inc., Norcross, GA. Element compositions are within ±0.4% of the calculated values. Fractional moles of water or organic solvents frequently found in some analytical samples of antifolates could not be prevented despite 24−48 h of drying in vacuo and were confirmed where possible by their presence in the ^{1}H NMR spectra. High-resolution mass spectrometry (HRMS) was performed on Waters Q-TOF (API-US) by Department of Chemistry, University of Pittsburgh, Pittsburgh, PA. Elemental analysis was used to determine the purity of the final compounds **1**−**3**. All solvents and chemicals were purchased from Aldrich Chemical Co. and Fisher Scientific and were used as received. Purity of the final compounds **1**−**3**, **7**−**9**, **10a**, and **10b** were >95% and were determined by elemental (C, H, N, S) analysis.

General Procedure for the Synthesis of Compounds 13a−b. To a 20 mL vial for microwave reaction were added a mixture of palladium chloride (71 mg, 0.40 mmol), triphenylphosphine (131 mg, 0.40 mmol), triethylamine (10.1 g, 100 mmol), 5-bromo-thiophene-2-carboxylic acid methyl ester, **12** (2.21 g, 10 mmol), and anhydrous acetonitrile (10 mL). To the stirred mixture were added copper(I) iodide (304 mg, 1.60 mmol) and prop-2-yn-1-ol, **11a**, or but-3-yn-1-ol, **11b** (1.05 equiv), and the vial was sealed and put into the microwave reactor at 100 °C for 10 min. Silica gel (5 g) was added, and the solvent was evaporated under reduced pressure. The resulting plug was loaded on to a silica gel column (3.5 × 12 cm) and eluted with hexane followed by 20% EtOAc in hexane. The desired fraction (TLC) was collected, and the solvent was evaporated under reduced pressure to afford **13a**−**b**.

*5-(3-Hydroxy-prop-1-ynyl)-thiophene-2-carboxylic Acid Methyl Ester (**13a**).* Compound **13a** was prepared using the general method described for the preparation of **13a**−**b**, from prop-2-yn-1-ol, **11a** (588 mg, 10.5 mmol), to give 1.45 g (74%) of **13a** as a yellow oil. TLC R_f 0.33 (hexane/EtOAc 1:1). ^{1}H NMR (DMSO-d_6): δ 3.82 (s, 3H, $COOCH_3$), 4.33−4.34 (d, J = 6.0 Hz, 2H, CH_2), 5.45−5.48 (t, J = 6.0 Hz, 1H, OH, exch), 7.34−7.35 (d, J = 4.0 Hz, 1H, Ar), 7.72−7.73 (d, J = 4.0 Hz, 1H, Ar).

*5-(4-Hydroxy-but-1-ynyl)-thiophene-2-carboxylic Acid Methyl Ester (**13b**).* Compound **13b** was prepared using the general method described for the preparation of **13a**−**b**, from prop-2-yn-1-ol, **11b** (588 mg, 8.4 mmol), to give 1.17 g (70%) of **13b** as a yellow oil. TLC R_f 0.33 (hexane/EtOAc 1:1). ^{1}H NMR (DMSO-d_6): δ 2.59−2.63 (t, J = 6.4 Hz, 2H, CH_2), 3.56−3.59 (t, J = 6.4 Hz, 2H, CH_2), 3.81 (s, 3H, $COOCH_3$), 4.95−4.98 (t, J = 5.6 Hz, 1H, OH, exch), 7.27−7.28 (d, J = 4.0 Hz, 1H, Ar), 7.69−7.70 (d, J = 4.0 Hz, 1H, Ar).

General Procedure for the Synthesis of Compounds 14a−b. To a Parr flask was added **13a**−**b**, 10% palladium on activated carbon (50% w/w), and MeOH (100 mL). Hydrogenation was carried out at 55 psi of H_2 for 4 h. The reaction mixture was filtered through Celite, washed with MeOH (100 mL), and concentrated under reduced pressure to give **14a**−**b**.

*5-(3-Hydroxy-propyl)-thiophene-2-carboxylic Acid Methyl Ester (**14a**).* Compound **14a** was prepared using the general method described for the preparation of **14a**−**b**, from **13a** (1.45 g, 7.4 mmol) to give 1.4 g (95%) of **14a** as a yellow oil. TLC R_f 0.34 (hexane/EtOAc 1:1). ^{1}H NMR (DMSO-d_6): δ 1.86−1.93 (m, 2H, CH_2), 2.68−2.71 (t, J = 6.8 Hz, 2H, CH_2), 3.06−3.09 (t, J = 6.8 Hz, 2H, CH_2), 3.76 (s, 3H, $COOCH_3$), 4.02−4.05 (t, J = 6.0 Hz, 1H, OH, exch), 6.97−6.98 (d, J = 4.0 Hz, 1H, Ar), 7.61−7.63 (d, J = 4.0 Hz, 1H, Ar).

*5-(4-Hydroxy-butyl)-thiophene-2-carboxylic Acid Methyl Ester (**14b**).* Compound **14b** was prepared using the general method described for the preparation of **14a**−**b**, from **13b** (1.17 g, 5.6 mmol) to give 1.14 g (95%) of **14b** as a yellow oil. TLC R_f 0.34 (hexane/EtOAc 1:1). ^{1}H NMR (DMSO-d_6): δ 1.41−1.48 (m, 2H, CH_2), 1.61−1.68 (m, 2H, CH_2), 2.81−2.85 (t, J = 7.2 Hz, 2H, CH_2), 3.37−3.42 (m, 2H, CH_2), 3.77 (s, 3H, $COOCH_3$), 4.40−4.43 (t, J = 5.2 Hz, 1H, OH, exch), 6.94−6.95 (d, J = 3.6 Hz, 1H, Ar), 7.63−7.64 (d, J = 3.6 Hz, 1H, Ar).

General Procedure for the Synthesis of Compounds 15b−c. To a solution of **14a**−**b** in acetone (15 mL) was added dropwise a cold solution (ice bath) of CrO_3 (6 equiv) in sulfuric acid (30 mL) and water (90 mL). After the addition, the resulting solution was stirred in an ice bath for an additional 2 h, and the solution was allowed to warm to room temperature overnight. The solution was extracted with 5 × 30 mL of ethyl ether and dried over Na_2SO_4. After evaporation of the solvent under reduced pressure, the resulting residue was flash chromatographed through a silica gel column (3.5 × 15 cm) using hexane/EtOAc (2:1) as eluent. The desired fraction (TLC) was collected, and the solvent was evaporated under reduced pressure to afford **15b**−**c**.

*5-(2-Carboxy-ethyl)-thiophene-2-carboxylic Acid Methyl Ester (**15b**).* Compound **15b** was prepared using the general method described for the preparation of **15b**−**c**, from **14a** (1.4 g, 7.0 mmol) to give 642 mg (43%) of **15b** as a colorless oil. TLC R_f 0.55 (hexane/EtOAc 1:1). ^{1}H NMR (DMSO-d_6): δ 2.59−2.62 (t, J = 7.2 Hz, 2H, CH_2), 3.03−3.07 (t, J = 7.2 Hz, 2H, CH_2), 3.78 (s, 3H, $COOCH_3$), 6.97−6.98 (d, J = 3.6 Hz, 1H, Ar), 7.62−7.63 (d, J = 3.6 Hz, 1H, Ar), 12.32 (br, 1H, COOH, exch).

*5-(3-Carboxy-propyl)-thiophene-2-carboxylic Acid Methyl Ester (**15c**).* Compound **15c** was prepared using the general method described for the preparation of **15b**−**c**, from **14b** (1.14 g, 5.3 mmol) to give 570 mg (47%) of **15c** as a colorless oil. TLC R_f 0.58 (hexane/EtOAc 1:1). ^{1}H NMR (DMSO-d_6): δ 1.79−1.87 (m, 2H, CH_2), 2.24−2.27 (t, J = 7.2 Hz, 2H, CH_2), 2.82−2.86 (t, J = 7.2 Hz, 2H, CH_2), 3.77 (s, 3H, $COOCH_3$), 6.95−6.96 (d, J = 3.6 Hz, 1H, Ar), 7.63−7.64 (d, J = 3.6 Hz, 1H, Ar), 12.17 (br, 1H, COOH, exch). HRMS calcd for $C_{10}H_{12}O_4S$ 228.0456; found, 228.0458.

General Procedure for the Synthesis of Compounds 16b−c. To **15b**−**c** in a 100 mL flask was added oxalyl chloride (6 equiv) and anhydrous CH_2Cl_2 (20 mL). The resulting solution was refluxed for 1 h and then cooled to room temperature. After evaporating the solvent under reduced pressure, the residue was dissolved in 20 mL of Et_2O. The resulting solution was added dropwise to ice-cooled diazomethane (generated in situ from 10 g of diazald by using Aldrich Mini Diazald Apparatus) in an ice bath over 10 min. The resulting mixture was allowed to stand for 30 min and then stirred for an additional 1 h. To this solution was added 48% HBr (20 mL). The resulting mixture was refluxed for 1.5 h. After cooling to room temperature, the organic layer was separated, and the aqueous layer was extracted with Et_2O (2 × 50 mL). The combined organic layer and Et_2O extract was washed with two portions of 10% Na_2CO_3 solution and dried over Na_2SO_4. Evaporation of the solvent under reduced pressure afforded **16b**−**c**.

*5-(4-Bromo-3-oxo-butyl)-thiophene-2-carboxylic Acid Methyl Ester (**16b**).* Compound **16b** was prepared using the general method described for the preparation of **16b**−**c**, from **15b** (642 mg, 3.0 mmol) to give 803 mg (92%) of **16b** as a colorless oil. TLC R_f 0.68 (hexane/EtOAc 1:1). ^{1}H NMR (DMSO-d_6): δ 3.00−3.06 (m, 4H, CH_2CH_2), 3.78 (s, 3H, $COOCH_3$), 4.37 (s, 2H, CH_2Br), 6.96−6.97 (d, J = 3.6 Hz, 1H, Ar), 7.62−7.63 (d, J = 3.6 Hz, 1H, Ar).

*5-(5-Bromo-4-oxo-pentyl)-thiophene-2-carboxylic Acid Methyl Ester (**16c**).* Compound **16c** was prepared using the general method described for the preparation of **16b**−**c**, from **15c** (570 mg, 2.5 mmol) to give 730 mg (96%) of **16c** as a colorless oil. TLC R_f 0.71 (hexane/EtOAc 1:1).

^{1}H NMR ($CDCl_3$-*d*): δ 1.99−2.07 (m, 2H, CH_2), 2.71−2.75 (t, *J* = 7.2 Hz, 2H, CH_2), 2.87−2.91 (t, *J* = 7.2 Hz, 2H, CH_2), 3.87 (s, 3H, $COOCH_3$), 3.88 (s, 2H, CH_2Br), 6.81−6.82 (d, *J* = 3.6 Hz, 1H, Ar), 7.64−7.65 (d, *J* = 3.6 Hz, 1H, Ar). HRMS calcd for $C_{11}H_{13}BrO_3S$ 303.9769; found, 303.9759.

Methyl 5-[(2-Amino-4-oxo-4,7-dihydro-3*H*-pyrrolo[2,3-*d*]pyrimidin-6-yl)methyl]thiophene-2-carboxylate (18a). To commercially available 5-carboxymethyl-thiophene-2-carboxylic acid methyl ester **15a** (1 g, 5.0 mmol) in a 100 mL flask was added oxalyl chloride (3.8 g, 30 mmol) and anhydrous CH_2Cl_2 (20 mL). The resulting solution was refluxed for 1 h and then cooled to room temperature. After evaporating the solvent under reduced pressure, the residue was dissolved in 20 mL of Et_2O. The resulting solution was added dropwise to ice-cooled diazomethane (generated in situ from 10 g of diazald by using Aldrich Mini Diazald Apparatus) in an ice bath over 10 min. The resulting mixture was allowed to stand for 30 min and then stirred for an additional 1 h. To this solution was added 48% HBr (20 mL). The resulting mixture was refluxed for 1.5 h. After cooling to room temperature, the organic layer was separated, and the aqueous layer was extracted with Et_2O (2 × 50 mL). The combined organic layer and Et_2O extract was washed with two portions of 10% Na_2CO_3 solution and dried over Na_2SO_4. To this residue in anhydrous DMF (15 mL) was added 2,6-diamino-3*H*-pyrimidin-4-one, **17** (630 mg, 5 mmol). The resulting mixture was stirred under N_2 at room temperature for 3 days. Silica gel (1.6 g) was then added, and the solvent was evaporated under reduced pressure. The resulting plug was loaded on to a silica gel column (1.5 × 12 cm) and eluted with $CHCl_3$ followed by 3% MeOH in $CHCl_3$ and then 5% MeOH in $CHCl_3$. The desired fraction (TLC) was collected, and the solvent was evaporated under reduced pressure to afford 180 mg (12%) of **18a** as a light yellow powder. Mp 200−201 °C; TLC R_f 0.18 ($CHCl_3$/MeOH 10:1). ^{1}H NMR (DMSO-d_6): δ 3.78 (s, 3H, $COOCH_3$), 4.10 (s, 2H, CH_2), 6.01 (s, 1H, C5-CH), 6.05 (s, 2H, 2-NH_2, exch), 7.00−7.01 (d, *J* = 4.0 Hz, 1H, Ar), 7.65−7.66 (d, *J* = 4.0 Hz, 1H, Ar), 10.21 (s, 1H, 3-NH, exch), 11.04 (s, 1H, 7-NH, exch).

General Procedure for the Synthesis of Compounds 18b−c. To a suspension of 2,6-diamino-3*H*-pyrimidin-4-one, **17** (1 equiv), in anhydrous DMF (15 mL) was added **16b−c**. The resulting mixture was stirred under N_2 at room temperature for 3 days. Silica gel (1.6 g) was then added, and the solvent was evaporated under reduced pressure. The resulting plug was loaded on to a silica gel column (1.5 × 12 cm) and eluted with $CHCl_3$ followed by 3% MeOH in $CHCl_3$ and then 5% MeOH in $CHCl_3$. The desired fraction (TLC) was collected, and the solvent was evaporated under reduced pressure to afford **18b−c**.

*Methyl 5-[(2-Amino-4-oxo-4,7-dihydro-3H-pyrrolo[2,3-d]pyrimidin-6-yl)ethyl]thiophene-2-carboxylate (**18b**).* Compound **18b** was prepared using the general method described for the preparation of **18b−c**, from **16b** (803 mg, 2.8 mmol) to give 320 mg (36%) of **18b** as a light yellow powder. Mp 200−201 °C; TLC R_f 0.18 ($CHCl_3$/MeOH 10:1). ^{1}H NMR (DMSO-d_6): δ 2.84−2.87 (t, *J* = 7.2 Hz, 2H, CH_2), 3.15−3.17 (t, *J* = 7.2 Hz, 2H, CH_2), 3.77 (s, 3H, $COOCH_3$), 5.91 (s, 1H, C5-CH), 6.09 (s, 2H, 2-NH_2, exch), 6.95−6.96 (d, *J* = 3.6 Hz, 1H, Ar), 7.61−7.62 (d, *J* = 3.6 Hz, 1H, Ar), 10.24 (s, 1H, 3-NH, exch), 10.94 (s, 1H, 7-NH, exch).

*Methyl 5-[(2-Amino-4-oxo-4,7-dihydro-3H-pyrrolo[2,3-d]pyrimidin-6-yl)propyl]thiophene-2-carboxylate (**18c**).* Compound **18c** was prepared using the general method described for the preparation of **18b−c**, from **16c** (730 mg, 2.4 mmol) to give 300 mg (38%) of **18c** as a white powder. Mp 175−176 °C; TLC R_f 0.17 ($CHCl_3$/MeOH 10:1). ^{1}H NMR (DMSO-d_6): δ 1.89−1.97 (m, 2H, CH_2), 2.49−2.54 (t, *J* = 7.2 Hz, 2H, CH_2), 2.82−2.85 (t, *J* = 7.2 Hz, 2H, CH_2), 3.78 (s, 3H, $COOCH_3$), 5.89 (s, 1H, C5-CH), 5.96 (s, 2H, 2-NH_2, exch), 6.97−6.98 (d, *J* = 3.6 Hz, 1H, Ar), 7.64−7.65 (d, *J* = 3.6 Hz, 1H, Ar), 10.13 (s, 1H, 3-NH, exch), 10.82 (s, 1H, 7-NH, exch).

General Procedure for the Synthesis of Compounds 19a−c. To a solution of **18a−c** in 10 mL of MeOH was added 1 N NaOH (10 mL), and the mixture was stirred under N_2 at room temperature for 16 h. TLC showed the disappearance of the starting material and one major spot at the origin. The reaction mixture was evaporated to dryness under reduced pressure. The residue was dissolved in water (10 mL), the resulting solution was cooled in an ice bath, and the pH was adjusted to 3−4 with dropwise addition of 1 N HCl. The resulting suspension was frozen in a dry ice−acetone bath, thawed to 4−5 °C in the refrigerator, and filtered. The residue was washed with a small amount of cold water and dried in vacuum using P_2O_5 to afford **19a−c**.

*5-[(2-Amino-4-oxo-4,7-dihydro-3H-pyrrolo[2,3-d]pyrimidin-6-yl)-methyl)thiophene-2-carboxylic Acid (**19a**).* Compound **19a** was prepared using the general method described for the preparation of **19a−c**, from **18a** (180 mg, 0.6 mmol) to give 163 mg (95%) of **19a** as a white powder. Mp 200−201 °C. ^{1}H NMR (DMSO-d_6): δ 4.08 (s, 2H, CH_2), 6.00 (s, 1H, C5-CH), 6.06 (s, 2H, 2-NH_2, exch), 6.96−6.97 (d, *J* = 4.0 Hz, 1H, Ar), 7.56−7.57 (d, *J* = 4.0 Hz, 1H, Ar), 10.22 (s, 1H, 3-NH, exch), 11.03 (s, 1H, 7-NH, exch), 12.97 (br, 1H, COOH, exch).

*5-[(2-Amino-4-oxo-4,7-dihydro-3H-pyrrolo[2,3-d]pyrimidin-6-yl)-ethyl)thiophene-2-carboxylic Acid (**19b**).* Compound **19b** was prepared using the general method described for the preparation of **19a−c**, from **18b** (320 mg, 1.0 mmol) to give 274 mg (90%) of **19b** as a white powder. Mp 200−201 °C. ^{1}H NMR (DMSO-d_6): δ 2.82−2.86 (t, *J* = 7.2 Hz, 2H, CH_2), 3.12−3.16 (t, *J* = 7.2 Hz, 2H, CH_2), 5.90 (s, 1H, C5-CH), 6.01 (s, 2H, 2-NH_2, exch), 6.89−6.90 (d, *J* = 3.6 Hz, 1H, Ar), 7.50−7.51 (d, *J* = 3.6 Hz, 1H, Ar), 10.18 (s, 1H, 3-NH, exch), 10.89 (s, 1H, 7-NH, exch), 12.90 (br, 1H, COOH, exch).

*5-[(2-Amino-4-oxo-4,7-dihydro-3H-pyrrolo[2,3-d]pyrimidin-6-yl)-propyl)thiophene-2-carboxylic Acid (**19c**).* Compound **19c** was prepared using the general method described for the preparation of **19a−c**, from **18c** (300 mg, 0.9 mmol) to give 254 mg (89%) of **19c** as a white powder. Mp 175−176 °C. ^{1}H NMR (DMSO-d_6): δ 1.89−1.96 (m, 2H, CH_2), 2.49−2.55 (t, *J* = 7.2 Hz, 2H, CH_2), 2.80−2.84 (t, *J* = 7.2 Hz, 2H, CH_2), 5.88 (s, 1H, C5-CH), 5.98 (s, 2H, 2-NH_2, exch), 6.92−6.93 (d, *J* = 3.6 Hz, 1H, Ar), 7.55−7.56 (d, *J* = 3.6 Hz, 1H, Ar), 10.14 (s, 1H, 3-NH, exch), 10.83 (s, 1H, 7-NH, exch), 12.86 (br, 1H, COOH, exch).

Diethyl *N*-({5-[(2-Amino-4-oxo-4,7-dihydro-3*H*-pyrrolo-[2,3-*d*]pyrimidin-6-yl)methyl]thiophen-2-yl}carbonyl)-L-glutamate (20a). To a solution of **19a** (118 mg, 0.4 mmol) in anhydrous DMF (10 mL) was added *N*-methylmorpholine (73 mg, 0.72 mmol) and 2-chloro-4,6-dimethoxy-1,3,5-triazine (127 mg, 0.72 mmol). The resulting mixture was stirred at room temperature for 2 h. To this mixture was added *N*-methylmorpholine (73 mg, 0.72 mmol) and L-glutamate diethyl ester hydrochloride (144 mg, 0.6 mmol). The reaction mixture was stirred for an additional 4 h at room temperature. Silica gel (400 mg) was then added, and the solvent was evaporated under reduced pressure. The resulting plug was loaded on to a silica gel column (1.5 × 15 cm) with 5% $CHCl_3$ in MeOH as the eluent. Fractions that showed the desired spot (TLC) were pooled and the solvent evaporated to dryness to afford 120 mg (63%) of **20a** as a yellow powder. Mp 78−79 °C. ^{1}H NMR (DMSO-d_6): δ 1.14−1.20 (m, 6H, $COOCH_2CH_3$), 1.93−2.11 (m, 2H, β-CH_2), 2.40−2.43 (t, *J* = 7.2 Hz, 2H, γ-CH_2), 4.02−4.13 (m, 4H, $COOCH_2CH_3$), 4.31 (s, 2H, CH_2), 4.34−4.40 (m, 1H, α-CH), 6.07 (s, 1H, C5-CH), 6.94−6.95 (d, *J* = 4.0 Hz, 1H, Ar), 7.71−7.72 (d, *J* = 4.0 Hz, 1H, Ar), 8.66−8.68 (d, *J* = 7.2 Hz, 1H, CONH, exch), 11.18 (s, 1H, 3-NH, exch), 11.43 (s, 1H, 7-NH, exch).

Diethyl *N*-({5-[(2-Amino-4-oxo-4,7-dihydro-3*H*-pyrrolo-[2,3-*d*]pyrimidin-6-yl)propyl]thiophen-2-yl}carbonyl)-L-glutamate (20c). To a solution of **19c** (254 mg, 0.8 mmol) in anhydrous DMF (10 mL) was added *N*-methylmorpholine (145 mg, 1.44 mmol) and 2-chloro-4,6-dimethoxy-1,3,5-triazine (253 g, 1.44 mmol). The resulting mixture was stirred at room temperature for 2 h. To this mixture were added *N*-methylmorpholine (145 mg, 1.44 mmol) and L-glutamate diethyl ester hydrochloride (290 mg, 1.2 mmol). The reaction

mixture was stirred for an additional 4 h at room temperature and then evaporated to dryness under reduced pressure. The residue was dissolved in the minimum amount of $CHCl_3$/MeOH (4:1) and chromatographed on a silica gel column (2 × 15 cm) with 5% $CHCl_3$ in MeOH as the eluent. Fractions that showed the desired spot (TLC) were pooled, and the solvent evaporated to dryness to afford 252 mg (63%) of **20c** as a yellow powder. Mp 85−86 °C; TLC R_f 0.13 ($CHCl_3$/MeOH 10:1). ^{1}H NMR (DMSO-d_6): δ 1.14−1.21 (m, 6H, $COOCH_2CH_3$), 1.81−2.05 (m, 4H, β-CH_2, CH_2), 2.32−2.39 (t, J = 7.6 Hz, 2H, γ-CH_2), 2.49−2.52 (t, J = 7.2 Hz, 2H, CH_2), 2.78−2.81 (t, J = 7.2 Hz, 2H, CH_2), 4.02−4.07 (m, 4H, $COOCH_2CH_3$), 4.30−4.35 (m, 1H, α-CH), 5.88 (s, 1H, C5-CH), 5.94 (s, 2H, 2-NH_2, exch), 6.89−6.90 (d, J = 3.6 Hz, 1H, Ar), 7.68−7.69 (d, J = 3.6 Hz, 1H, Ar), 8.61−8.63 (d, J = 8 Hz, 1H, CONH, exch), 10.71 (s, 1H, 3-NH, exch), 11.19 (s, 1H, 7-NH, exch).

***N*-({5-[(2-Amino-4-oxo-4,7-dihydro-*3H*-pyrrolo[2,3-*d*]pyrimidin-6-yl)methyl]thiophen-2-yl}carbonyl)-L-glutamic Acid (1).** To a solution of **20a** (120 mg, 0.25 mmol) in MeOH (10 mL) was added 1 N NaOH (4 mL). The mixture was then stirred under N_2 at room temperature for 16 h. TLC showed the disappearance of the starting material (R_f 0.15) and one major spot at the origin ($CHCl_3$/MeOH 10:1). The reaction mixture was then evaporated to dryness under reduced pressure. The residue was dissolved in water (10 mL), the resulting solution was cooled in an ice bath, and the pH was adjusted to 3−4 with dropwise addition of 1 N HCl. The resulting suspension was frozen in a dry ice-acetone bath, thawed to 4−5 °C in the refrigerator, and filtered. The residue was washed with a small amount of cold water and dried in vacuum using P_2O_5 to afford 73 mg (69%) of **1** as a light yellow powder. Mp 167−168 °C. ^{1}H NMR (DMSO-d_6): δ 1.85−2.11 (m, 2H, β-CH_2), 2.31−2.35 (t, J = 6.8 Hz, 2H, γ-CH_2), 4.06 (s, 2H, CH_2), 4.30−4.36 (m, 1H, α-CH), 6.00 (s, 1H, C5-CH), 6.07 (s, 2H, 2-NH_2, exch), 6.92−6.93 (d, J = 4.0 Hz, 1H, Ar), 7.69−7.70 (d, J = 4.0 Hz, 1H, Ar), 8.52−8.54 (d, J = 8 Hz, 1H, CONH, exch), 10.22 (s, 1H, 3-NH, exch), 11.03 (s, 1H, 7-NH, exch), 12.46 (br, 2H, COOH, exch). Anal. ($C_{17}H_{17}N_5O_6S$) C, H, N, S.

***N*-({5-[(2-Amino-4-oxo-4,7-dihydro-*3H*-pyrrolo[2,3-*d*]pyrimidin-6-yl)ethyl]thiophen-2-yl}carbonyl)-L-glutamic Acid (2).** To a solution of **19b** (274 mg, 0.9 mmol) in anhydrous DMF (10 mL) was added *N*-methylmorpholine (164 mg, 1.62 mmol) and 2-chloro-4,6-dimethoxy-1,3,5-triazine (285 mg, 1.62 mmol). The resulting mixture was stirred at room temperature for 2 h. To this mixture was added *N*-methylmorpholine (164 mg, 1.62 mmol) and L-glutamate diethyl ester hydrochloride (324 mg, 1.35 mmol). The reaction mixture was stirred for an additional 4 h at room temperature. Silica gel (600 mg) was then added, and the solvent was evaporated under reduced pressure. The resulting plug was loaded on to a silica gel column (1.5 × 15 cm) with 5% $CHCl_3$ in MeOH as the eluent. Fractions that showed the desired spot (TLC) were pooled, and the solvent evaporated to dryness to afford a residue. To this residue was added MeOH (10 mL) and 1 N NaOH (10 mL), and the mixture was stirred under N_2 at room temperature for 16 h. TLC showed the disappearance of the starting material (R_f 0.15) and one major spot at the origin ($CHCl_3$/MeOH 10:1). The reaction mixture was then evaporated to dryness under reduced pressure. The residue was dissolved in water (10 mL), the resulting solution was cooled in an ice bath, and the pH was adjusted to 3−4 with dropwise addition of 1 N HCl. The resulting suspension was frozen in a dry ice-acetone bath, thawed to 4−5 °C in the refrigerator, and filtered. The residue was washed with a small amount of cold water and dried in vacuum using P_2O_5 to afford 262 mg (67%) of **2** as a light yellow powder. Mp 184−185 °C. ^{1}H NMR (DMSO-d_6): δ 1.84−2.10 (m, 2H, β-CH_2), 2.30−2.34 (t, J = 7.4 Hz, 2H, γ-CH_2), 2.81−2.85 (t, J = 7.4 Hz, 2H, CH_2), 3.10−3.13 (t, J = 7.4 Hz, 2H, CH_2), 4.29−4.35 (m, 1H, α-CH), 5.91 (s, 1H, C5-CH), 6.03 (s, 2H, 2-NH_2, exch), 6.87−6.88 (d, J = 3.6 Hz, 1H, Ar), 7.66−7.67 (d, J = 3.6 Hz, 1H, Ar), 8.49−8.51 (d, J = 8.0 Hz, 1H, CONH, exch), 10.18 (s, 1H, 3-NH, exch), 10.90 (s, 1H, 7-NH, exch), 12.41 (br, 2H, COOH, exch). Anal. ($C_{18}H_{19}N_5O_6S$) C, H, N, S.

***N*-({5-[(2-Amino-4-oxo-4,7-dihydro-*3H*-pyrrolo[2,3-*d*]pyrimidin-6-yl)propyl]thiophen-2-yl}carbonyl)-L-glutamic Acid (3).** To a solution of **20c** (252 mg, 0.5 mmol) in MeOH (10 mL) was added 1 N NaOH (10 mL), and the mixture was stirred under N_2 at room temperature for 16 h. TLC showed the disappearance of the starting material (R_f 0.13) and one major spot at the origin ($CHCl_3$/MeOH 10:1). The reaction mixture was evaporated to dryness under reduced pressure. The residue was dissolved in water (10 mL), the resulting solution was cooled in an ice bath, and the pH was adjusted to 3−4 with dropwise addition of 1 N HCl. The resulting suspension was frozen in a dry ice-acetone bath, thawed to 4−5 °C in the refrigerator, and filtered. The residue was washed with a small amount of cold water and dried in vacuum using P_2O_5 to afford 212 mg (95%) of **3** as white powder. Mp 168−169 °C. ^{1}H NMR (DMSO-d_6): δ 1.88−2.10 (m, 4H, β-CH_2, CH_2), 2.31−2.34 (t, J = 7.6 Hz, 2H, γ-CH_2), 2.49−2.54 (t, J = 7.2 Hz, 2H, CH_2), 2.78−2.81 (t, J = 7.2 Hz, 2H, CH_2), 4.30−4.35 (m, 1H, α-CH), 5.88 (s, 1H, C5-CH), 5.97 (s, 2H, 2-NH_2, exch), 6.89−6.90 (d, J = 3.6 Hz, 1H, Ar), 7.68−7.69 (d, J = 3.6 Hz, 1H, Ar), 8.50−8.52 (d, J = 8 Hz, 1H, CONH, exch), 10.13 (s, 1H, 3-NH, exch), 10.82 (s, 1H, 7-NH, exch), 12.42 (br, 2H, COOH, exch). Anal. ($C_{19}H_{21}N_5O_6S$) C, H, N, S.

Reagents for Biological Studies. [3′,5′,7-^{3}H]MTX (20 Ci/mmol), [3′,5′,7,9-^{3}H] folic acid (25 Ci/mmol), and [^{14}C(U)]-glycine (87mCi/mmol) were purchased from Moravek Biochemicals (Brea, CA). Unlabeled folic acid was purchased from the Sigma Chemical Co. (St. Louis, MO). LCV [(6*R*,*S*) 5-formyl tetrahydrofolate] was provided by the Drug Development Branch, National Cancer Institute, Bethesda, MD. The sources of the classical antifolate drugs were as follows: MTX, Drug Development Branch, National Cancer Institute (Bethesda, MD); RTX [*N*-(5-[*N*-(3,4-dihydro-2-methyl-4-oxyquinazolin-6-ylmethyl)-*N*-methyl-amino]-2-thienoyl)-L-glutamic acid], AstraZeneca Pharmaceuticals (Maccesfield, Cheshire, England); LMTX (5,10-dideaza-5,6,7,8-tetrahydrofolate) and PMX [*N*-{4-[2-(2-amino-3,4-dihydro-4-oxo-7*H*-pyrrolo[2,3-*d*]pyrimidin-5-yl)ethyl]benzoyl}-L-glutamic acid] (Alimta), Eli Lilly and Co. (Indianapolis, IN); and PT523 [N^{α}-(4-amino-4-deoxypteroyl)-N^{δ}-hemiphthaloyl-L-ornithine], Dr. Andre Rososky (Boston, MA). Other chemicals were obtained from commercial sources in the highest available purity.

Cell Lines and Assays of Antitumor Drug Activities. The engineered CHO sublines including RFC- and FRα-null MTXRIIOua^{R}2−4 (R2), and hRFC (PC43-10)-, hPCFT (R2/PCFT4)-, or FRα (RT16) and FRβ (D4)-expressing CHO sublines were previously described.[12−15] The pcDNA3.1 vector transfected control CHO cells (R2/VC) were previously described.[14] The CHO cells were cultured in α-minimal essential medium (MEM) supplemented with 10% bovine calf serum (Invitrogen, Carlsbad, CA), penicillin−streptomycin solution, and L-glutamine at 37 °C with 5% CO_2. All the R2 transfected cells [PC43-10, RT16, D4, R2/hPCFT4, and R2(VC)] were routinely cultured in α-MEM plus 1.5 mg/mL G418.[14−16] Prior to the cell proliferation assays (see below), RT16 and D4 cells were cultured for 3 days in complete folate-free RPMI 1640 (without added folate) with dFBS plus 1.5 mg/mL G418. KB human cervical cancer cells were purchased from the American Type Culture Collection (Manassas, VA), whereas IGROV1 ovarian carcinoma cells were a gift of Dr. Manohar Ratnam (University of Toledo). Both IGROV1 and KB cells were routinely cultured in folate-free RPMI 1640 medium, supplemented with 10% fetal bovine serum, penicillin−streptomycin solution, and 2 mM L-glutamine at 37 °C with 5% CO_2.

For growth inhibition studies, cells (CHO, KB, or IGROV1) were plated in 96 well dishes (~2500−5000 cells/well, total volume of 200 μL medium) with various antifolate concentrations. The medium was standard RPMI 1640 with 10% dialyzed serum and antibiotics for experiments with R2 and PC43-10 cells. For experiments with RT16, D4, KB, and IGROV1 cells, the cells were cultured in a folate-free RPMI medium with 10% dFBS (Invitrogen) and antibiotics; the medium was

supplemented with 2 nM LCV. The requirement for FR-mediated drug uptake in these assays was established in parallel incubations including 200 nM folic acid, along with the cytotoxic antifolate. For the growth inhibition studies with R2/hPCFT4 cells, cells were cultured in folate-free RPMI 1640 (pH 7.2) containing 25 nM LCV, supplemented with 10% dFBS and antibiotics. Cells were routinely incubated for up to 96 h during which the medium pH decreased to ~6.8−6.9. Metabolically active cells (reflecting cell viability) were assayed with CellTiter-blue Cell Viability Assay (Promega, Madison, WI), with fluorescence measured (590 nm emission, 560 nm excitation) using a fluorescence plate reader. Raw data were exported from Softmax Pro software to an Excel spreadsheet for determinations of IC_{50}s, corresponding to the drug concentrations that result in 50% loss of cell growth.

For some of the in vitro growth inhibition studies, inhibitory effects of the antifolate drugs on de novo thymidylate synthase and de novo purine nucleotide biosynthesis (GARFTase and AICARFTase) were tested by coincubations with thymidine (10 μM) and adenosine (60 μM), respectively. For de novo purine biosynthesis, additional protection experiments used AICA (320 μM) to distinguish inhibitory effects at GARFTase from those at AICARFTase.[12−14]

For assays of colony formation in the presence of the antifolate drugs, R2/hPCFT4 cells were harvested and diluted, and 200 cells were plated into 60 mm dishes in a folate-free RPMI1640 medium supplemented with 25 nM LCV, 10% dFBS, penicillin−streptomycin, and 2 mM L-glutamine, in the presence of antifolate drugs. The dishes were incubated at 37 °C with 5% CO_2 for 10−14 days. At the end of the incubations, the dishes were rinsed with Dulbecco's phosphate-buffered saline (DPBS), 5% trichloroacetic acid, and borate buffer (10 mM, pH 8.8), followed by a 30 min incubation in 1% methylene blue in borate buffer. The dishes were rinsed with borate buffer, and colonies were counted for calculating the percent colony-forming efficiency normalized to control.

FR Binding Assay. [^{3}H]Folic acid binding was used to evaluate binding affinities.[12] Briefly, RT16 and D4 cells (~1.6×10^6) were rinsed twice with DPBS, followed by two washes with an acidic buffer (10 mM sodium acetate, 150 mM NaCl, pH 3.5) to remove FR-bound folates. Cells were washed twice with ice-cold HEPES-buffered saline (20 mM HEPES, 140 mM NaCl, 5 mM KCl, 2 mM $MgCl_2$, and 5 mM glucose, pH 7.4) (HBS), then incubated in HBS with [^{3}H]folic acid (50 nM, specific activity 0.5 Ci/mmol) in the presence and absence of unlabeled folic acid or antifolate (over a range of concentrations) for 15 min at 0 °C. The dishes were rinsed (3×) with ice-cold HBS after which the cells were solubilized (0.5 N NaOH), and aliquots of the alkaline homogenates were measured for radioactivity and protein contents. Protein concentrations were measured with Folin-phenol reagent.[28] Bound [^{3}H]folic acid was calculated as picomoles per milligram of protein, and relative binding affinities were calculated as the inverse molar ratios of unlabeled ligands required to inhibit [^{3}H]folic acid binding by 50%. By definition, the relative affinity for folic acid is 1.

Transport Assays. For membrane transport assays, R2/hPCFT4, PC43-10, and R2(VC) CHO cells were grown as monolayers and used to seed spinner flasks. For experiments to determine the inhibitions of transport by antifolate substrates, cells were collected and washed with DPBS and resuspended in 2 mL of physiologic Hank's balanced salts solution (HBSS) for PC43-10 cells, and in HBS, adjusted to pH 7.2 or 6.8, or in 4-morpholinepropanesulfonic acid (MES)-buffered saline (20 mM MES, 140 mM NaCl, 5 mM KCl, 2 mM $MgCl_2$, and 5 mM glucose), adjusted to pH 6.5, 6.0, or 5.5, for R2/hPCFT4 cells. Uptakes of [^{3}H]MTX (0.5 μM) were measured over 2 min at 37 °C, in the presence and absence of unlabeled antifolates (10 μM). Uptakes of [^{3}H]MTX were quenched with ice-cold DPBS. Cells were washed with ice-cold DPBS (3×) and solubilized with 0.5 N NaOH. Levels of intracellular radioactivity were expressed as picomoles per milligram of protein, calculated from direct measurements of radioactivity and protein contents of cell homogenates. Protein concentrations were measured with Folin-phenol reagent.[28] Percent MTX transport inhibition was calculated by comparing the levels of [^{3}H]MTX uptake in the presence and absence of the inhibitors. Kinetic constants (K_t, V_{max}) and K_is were calculated from Lineweaver−Burke and Dixon plots, respectively. These methods are analogous to those previously published.[13−15]

Electrophysiology Experiments. *Xenopus* oocytes were used to determine the currents associated with the transport of the antifolate substrates. Briefly, hPCFT cRNA (50 nL of 0.5 μg/μL, i.e., 25 ng) or water (50 nL) was injected into stage V/VI oocytes and electrophysiological measurements were recorded 3−5 days later.[15,25] Oocytes were voltage clamped to −90 mV to maximize folate-induced currents, a technique that was previously used in studies on the divalent metal transporter, DMT1,[29,30] and PCFT.[15,16] Oocyte solutions were adjusted to pH 5.5 using MES (pH 5.5). During these experiments, oocytes were continuously superfused with solution (with and without substrates as indicated) at 5 mL/min.

In Situ GARFTase Enzyme Inhibition Assay. To measure intracellular GARFTase activity in R2/hPCFT4 cells, we measured the incorporation of [^{14}C(U)]glycine into [^{14}C]formyl β-glycinamide ribonucleotide (GAR).[15] Briefly, R2/hPCFT4 cells were seeded in 5 mL of folate-free RPMI 1640 plus 25 nM LCV, 10% dFBS, and 2 mM L-glutamine and penicillin−streptomycin in T25 flasks at a density of 2×10^5 cells per flask. After 48 h, antifolate inhibitor or DMSO (control) was added to the culture medium. The cells were incubated for another 15 h (the pH was ~6.9 at this time). Cells were washed (2×) with DPBS and resuspended in 5 mL of folate-free, L-glutamine-free RPMI 1640 plus penicillin−streptomycin, 10% dFBS, 0.46 g/L $NaHCO_3$, and 1.21 g/L NaCl medium, with or without 0.5−100 nM antifolate and azaserine (4 μM final concentration), and incubated for 30 min. L-Glutamine (2 mM final concentration) and [^{14}C]glycine (final specific activity, 0.1 mCi/L) were added; cells were incubated at 37 °C for 8 h after which time the cells were trypsinized and washed twice with ice-cold DPBS. Cell pellets were treated with 2 mL of 5% trichloroacetic acid at 0 °C. Cell debris was removed by centrifugation, and samples were solubilized in 0.5 N NaOH and assayed for protein contents.[28] The supernatants were extracted twice with 2 mL of ice-cold ether to remove the trichloroacetic acid. The aqueous layer was passed through a 1 cm column of AG1x8 (chloride form, 100−200 mesh) (BioRad), washed with 10 mL of 0.5 N formic acid, followed by 10 mL of 4 N formic acid, and eluted with 8 mL of 1 N HCl solution. The eluants were collected as 1 mL fractions and determined for radioactivity. The accumulation of [^{14}C]formyl GAR was calculated as picomoles per milligram of protein over a range of inhibitor concentrations. IC_{50}s were calculated as the concentrations of inhibitors that resulted in a 50% decrease in [^{14}C]formyl GAR synthesis.

Measurement of Intracellular ATP Levels. For analysis of ATP levels following antifolate treatments, R2/hPCFT4 cells were seeded in 10 mL of folate-free RPMI 1640, 10% dFBS, 2 mM L-glutamine and penicillin-streptomycin plus 25 nM leucovorin (pH 7.2), then replaced after 24 h with the same media buffered to pH 6.8 with 25 mM PIPES/25 mM HEPES. Antifolates, including **3**, **4**, PMX, or LMTX (each at 1 μM), or vehicle (0.5% DMSO for **3** and **4**, H_2O for PMX and LMTX) (controls) were added to the culture medium. Cells were incubated for an additional 24 h after which they were trypsinized and washed (2×) with ice-cold DPBS. Nucleotides were extracted, and ATP levels were quantitated by HPLC exactly as previously described.[15]

In Vivo Efficacy Study in IGROV1 Cells. The methods for protocol design, drug treatment, toxicity evaluation, data analysis, quantification of tumor cell kill, tumor model systems, and the biological significance of the drug treatment results with transplantable tumors have been described previously.[14,31−35] Cultured IGROV1 human ovarian tumor cells were grown in folate-deficient media and were implanted subcutaneously (5×10^6 cells/flank) to establish a solid tumor xenograft model in female ICR SCID mice (obtained from

Taconic Laboratories). For the efficacy study, mice were 10 weeks old on day 0 (tumor implant) with an average body weight of 25.9 g. Mice were supplied food and water ad libitum. Study mice were maintained on either a folate-deficient diet from Harlan-Teklad (TD.00434) or a folate-replete diet from Lab Diet (5021; autoclavable mouse breeder diet) starting 24 days before the subcutaneous tumor implant to ensure serum folate levels would approximate those of humans. Folate serum levels were determined prior to tumor implant and post study via *L. casei* bioassay.[36] The animals were pooled and implanted bilaterally subcutaneously with 30 to 60 mg tumor fragments by a 12 gauge trocar and again pooled before unselective distribution to the various treatment and control groups. Chemotherapy began 3 days after tumor implantation, when the number of cells was relatively small (10^7 to 10^8 cells; before the established limit of palpation). Tumors were measured with a caliper two or three times weekly (depending on the doubling time of the tumor). Mice were sacrificed when the cumulative tumor burden reached 1500 mg. Tumor weights were estimated from two-dimensional measurements [i.e., tumor mass (in mg) = $(a \times b^2)/2$, where a and b are the tumor length and width in mm, respectively]. For the calculation of end points, both tumors on each mouse were added together, and the total mass per mouse was used. The following quantitative end-points were used to assess antitumor activity: (i) T/C [where T is the median time in days required for the treatment group tumors to reach a predetermined size (e.g., 1000 mg), and C is the median time in days for the control group tumors to reach the same size; tumor-free survivors are excluded from these calculations]; and (ii) tumor cell kill [$\log_{10}$ cell kill total (gross) = $(T - C)/(3.32)(T_d)$, where $T - C$ is the tumor growth delay, and T_d is the tumor volume doubling time in days, estimated from the best fit straight line from a log−linear growth plot of control group tumors in exponential growth (100 to 800 mg range)].

■ ASSOCIATED CONTENT

Supporting Information. Preliminary toxicity and antitumor efficacy evaluation, elemental analysis, and high-resolution mass spectra (HRMS) (ESI). This material is available free of charge via the Internet at http://pubs.acs.org.

■ AUTHOR INFORMATION

Corresponding Author

*Tel: 313-578-4280. Fax: 313-578-4287. E-mail: matherly@kci.wayne.edu (L.H.M.). Tel: 412-396-6070. Fax: 412-396-5593. E-mail: gangjee@duq.edu (A.G.).

Author Contributions

▽These authors contributed equally to this work.

■ ACKNOWLEDGMENT

This work was supported, in part, by grants from the National Institutes of Health, National Cancer Institute, CA125153 (to A.G.), CA152316 (to L.H.M. and A.G.), and CA53535 (to L.H.M.), a grant from the Mesothelioma Applied Research Foundation, a pilot grant from the Barbara Ann Karmanos Cancer Institute, and support from the Duquesne University Adrian Van Kaam Chair in Scholarly Excellence (A.G.). S.K.D. was supported by a Doctoral Research Award from the Canadian Institutes of Health Research (CIHR).

■ ABBREVIATIONS USED

AICA, 5-amino-4-imidazolecarboxamide; AICAR, 5-amino-4-imidazolecarboxamide ribonucleotide; AICARFTase, 5-amino-4-imidazolecarboxamide ribonucleotide formyltransferase; CHO, Chinese hamster ovary; dFBS, dialyzed fetal bovine serum; DPBS, Dulbecco's phosphate-buffered saline; FGAR, formyl glycinamide ribonucleotide; FR, folate receptor; GAR, glycinamide ribonucleotide; GARFTase, glycinamide ribonucleotide formyltransferase; HBSS, Hank's balanced salts solution; HBS, HEPES-buffered saline; hPCFT, human PCFT; hRFC, human RFC; LCV, Leucovorin; LMTX, lometrexol; MTX, methotrexate; PMX, pemetrexed; PCFT, proton-coupled folate transporter; RTX, raltitrexed; RFC, reduced folate carrier; SCID, severe combined immunodeficient

■ REFERENCES

(1) Chabner, B. A.; Allegra, C. Antifolates. In *Cancer Chemotherapy and Biotherapy: Principles and Practice*; Chabner, B. A., Longo, D. L., Eds.; Lippincott Williams and Wilkins: Philadelphia, PA, 2011; pp 109−138.

(2) Matherly, L. H.; Hou, Z.; Deng, Y. Human Reduced Folate Carrier: Translation of Basic Biology to Cancer Etiology and Therapy. *Cancer Metastasis Rev.* **2007**, *26*, 111–128.

(3) Zhao, R.; Goldman, I. D. Resistance to Antifolates. *Oncogene* **2003**, *22*, 7431–7457.

(4) Elnakat, H.; Ratnam, M. Distribution, Functionality and Gene Regulation of Folate Receptor Isoforms: Implications in Targeted Therapy. *Adv. Drug Delivery* **2004**, *56*, 1067–1084.

(5) Qiu, A.; Jansen, M.; Sakaris, A.; Min, S. H.; Chattopadhyay, S.; Tsai, E.; Sandoval, C.; Zhao, R.; Akabas, M. H.; Goldman, I. D. Identification of an Intestinal Folate Transporter and the Molecular Basis for Hereditary Folate Malabsorption. *Cell* **2006**, *127*, 917–928.

(6) Zhao, R.; Goldman, I. D. The Molecular Identity and Characterization of a Proton-Coupled Folate Transporter-PCFT; Biological Ramifications and Impact on the Activity of Pemetrexed. *Cancer Metastasis Rev.* **2007**, *26*, 129–139.

(7) Zhao, R.; Matherly, L. H.; Goldman, I. D. Membrane Transporters and Folate Homeostasis; Intestinal Absorption, Transport into Systemic Compartments and Tissues. *Expert Rev. Mol. Med.* **2009**, *11*, e4.

(8) Salazar, M. D.; Ratnam, M. The Folate Receptor: What Does It Promise in Tissue-Targeted Therapeutics? *Cancer Metastasis Rev.* **2007**, *26*, 141–152.

(9) Matherly, L. H.; Gangjee, A. Discovery of Novel Antifolate Inhibitors of de novo Purine Nucleotide Biosynthesis With Selectivity for High Affinity Folate Receptors and the Proton-coupled Folate Transporter Over the Reduced Folate Carrier for Cellular Entry. In *Targeted Drug Strategies for Cancer and Inflammation*; Jackman, A. L., Leamon, C., Eds.; Springer: New York, 2011, pp 119−134.

(10) Zhao, R.; Gao, F.; Hanscom, M.; Goldman, I. D. A Prominent Low-pH Methotrexate Transport Activity in Human Solid Tumors: Contribution to the Preservation of Methotrexate Pharmacologic Activity in HeLa Cells Lacking the Reduced Folate Carrier. *Clin. Cancer Res.* **2004**, *10*, 718–727.

(11) Gibbs, D. D.; Theti, D. S.; Wood, N.; Green, M.; Raynaud, F.; Valenti, M.; Forster, M. D.; Mitchell, F.; Bavetsias, V.; Henderson, E.; Jackman, A. L. BGC 945, a Novel Tumor-Selective Thymidylate Synthase Inhibitor Targeted to Alpha-Folate Receptor-Overexpressing Tumors. *Cancer Res.* **2005**, *65*, 11721–11728.

(12) Deng, Y.; Wang, Y.; Cherian, C.; Hou, Z.; Buck, S. A.; Matherly, L. H.; Gangjee, A. Synthesis and Discovery of High Affinity Folate Receptor-Specific Glycinamide Ribonucleotide Formyltransferase Inhibitors With Antitumor Activity. *J. Med. Chem.* **2008**, *51*, 5052–5063.

(13) Deng, Y.; Zhou, X.; Kugel Desmoulin, S.; Wu, J.; Cherian, C.; Hou, Z.; Matherly, L. H.; Gangjee, A. Synthesis and Biological Activity of a Novel Series of 6-Substituted Thieno[2,3-d]pyrimidine Antifolate Inhibitors of Purine Biosynthesis With Selectivity for High Affinity Folate Receptors Over the Reduced Folate Carrier and Proton-Coupled

Folate Transporter for Cellular Entry. *J. Med. Chem.* **2009**, *52*, 2940–2951.

(14) Wang, L.; Cherian, C.; Kugel Desmoulin, S.; Polin, L.; Deng, Y.; Wu, J.; Hou, Z.; White, K.; Kushner, J.; Matherly, L. H.; Gangjee, A. Synthesis and Antitumor Activity of a Novel Series of 6-substituted Pyrrolo[2,3-d]pyrimidine Thienoyl Antifolate Inhibitors of Purine Biosynthesis With Selectivity for High Affinity Folate Receptors and the Proton-coupled Folate Transporter Over the Reduced Folate Carrier for Cellular Entry. *J. Med. Chem.* **2010**, *53*, 1306–1318.

(15) Kugel Desmoulin, S.; Wang, Y.; Wu, J.; Stout, M.; Hou, Z.; Fulterer, A.; Chang, M. H.; Romero, M. F.; Cherian, C.; Gangjee, A.; Matherly, L. H. Targeting the Proton-coupled Folate Transporter for Selective Delivery of 6-Substituted Pyrrolo[2,3-*d*]Pyrimidine Antifolate Inhibitors of *de novo* Purine Biosynthesis in the Chemotherapy of Solid Tumors. *Mol. Pharmacol.* **2010**, *78*, 577–587.

(16) Rosowsky, A. PT523 and Other Aminopterin Analogs with a Hemiphthaloyl-L-ornithine Side Chain: Exceptionally Tight-Binding Inhibitors of Dihydrofolate Reductase Which Are Transported by the Reduced Folate Carrier but Cannot Form Polyglutamates. *Curr. Med. Chem.* **1999**, *6*, 329–352.

(17) Taylor, E. C.; Harrington, P. J.; Fletcher, S. R.; Beardsley, G. P.; Moran, R. G. Synthesis of the Antileukemic Agents 5,10-Dideazaaminopterin and 5,10-Dideaza-5,6,7,8-tetrahydroaminopterin. *J. Med. Chem.* **1985**, *28*, 914–921.

(18) Beardsley, G. P.; Moroson, B. A.; Taylor, E. C.; Moran, R. G. A New Folate Antimetabolite, 5,10-Dideaza-5,6,7,8-tetrahydrofolate Is a Potent Inhibitor of de Novo Purine Synthesis. *J. Biol. Chem.* **1989**, *264*, 328–333.

(19) Moran, R. G.; Baldwin, S. W.; Taylor, E. C.; Shih, C. The 6S- and 6R-Diastereomers of 5,10-Dideaza-5,6,7,8-tetrahydrofolate Are Equiactive Inhibitors of de Novo Purine Synthesis. *J. Biol. Chem.* **1989**, *264*, 21047–1051.

(20) Mendelsohn, L. G.; Worzalla, J. F.; Walling, J. M. Preclinical and Clinical Evaluation of the Glycinamide Ribonucleotide Formyltransferase Inhibitors Lometrexol and LY309887. In *Anticancer Drug Development Guide: Antifolate Drugs in Cancer Therapy*; Jackman, A. L., Ed.; Humana Press, Inc.: Totowa, NJ, 1999; pp 261−280.

(21) Budman, D. R.; Johnson, R.; Barile, B.; Bowsher, R. R.; Vinciguerra, V.; Allen, S. L.; Kolitz, J.; Ernest, C. S., II; Kreis, W.; Zervos, P.; Walling, J. Phase I and Pharmacokinetic Study of LY309887: A Specific Inhibitor of Purine Biosynthesis *Cancer Chemother. Pharmacol.* **2001**, *47*, 525–553.

(22) Boritzki, T. J.; Zhang, C.; Bartlett, C. A.; Jackson, R. C. AG2034 A GARFT Inhibitor With Selective Cytotoxicity to Cells that Lack a G1 Checkpoint. In *Anticancer Drug Development Guide: Antifolate Drugs in Cancer Therapy*; Jackman, A. L., Ed.; Humana Press Inc.: Totowa, NJ, 1999; pp 281− 292.

(23) Ray, M. S.; Muggia, F. M.; Leichman, G.; Grunberg, S. M.; Nelson, R. L.; Dyke, R. W.; Moran, R. G. Phase I Study of (6R)-5,10-Dideazatetrahydrofolate: A Folate Antimetabolite Inhibitory to De Novo Purine Synthesis. *J. Natl. Cancer Inst.* **1993**, *85*, 1154–1159.

(24) McLeod, H. L.; Cassidy, J.; Powrie, R. H.; Priest, D. G.; Zorbas, M. A.; Synold, T. W.; Shibata, S.; Spicer, D.; Bissett, D.; Pithavala, Y. K.; Collier, M. A.; Paradiso, L. J.; Roberts, J. D. Pharmacokinetic and Pharmacodynamic Evaluation of the Clycinamide Ribonucleotide Formyltransferase Inhibitor AG2034. *Clin. Cancer. Res.* **2000**, *6*, 2677–2684.

(25) Unal, E. S.; Zhao, R.; Chang, M. H.; Fiser, A.; Romero, M. F.; Goldman, I. D. The Functional Roles of the His247 and His281 Residues in Folate and Proton Translocation Mediated by the Human Proton-coupled Folate Transporter SLC46A1. *J. Biol. Chem.* **2009**, *284*, 17846–17857.

(26) Shih, C.; Thornton, D. E. Preclinical Pharmacology Studies on the Clinical Development of a Novel Multitargeted Antifolate, MTA (LY231514). In *Anticancer Development Guide: Antifolate Drugs in Cancer Therapy.*; Jackman, A. L. Ed.; Humana Press Inc.: Totowa, NJ, 1999; 183−201.

(27) Racanelli, A. C.; Rothbart, S. B.; Heyer, C. L.; Moran, R. G. Therapeutics by Cytotoxic Metabolite Accumulation: Pemetrexed Causes ZMP Accumulation, AMPK Activation, and Mammalian Target of Rapamycin Inhibition. *Cancer Res.* **2009**, 5467–5474.

(28) Lowry, O. H.; Rosebrough, N. J.; Farr, A. L.; Randall, R. J. Protein Measurement with the Folin Phenol Reagent. *J. Biol. Chem.* **1951**, *193*, 265–275.

(29) Gunshin, H.; Mackenzie, B.; Berger, U. V.; Gunshin, Y.; Romero, M. F.; Boron, W. F.; Nussberger, S.; Gollan, J. L.; Hediger, M. A. Cloning and Characterization of a Mammalian Proton-coupled Metal-ion Transporter. *Nature* **1997**, *388*, 482–488.

(30) Mackenzie, B.; Ujwal, M. L.; Chang, M. H.; Romero, M. F.; Hediger, M. A. Divalent Metal-ion Transporter DMT1 Mediates Both H^+-coupled Fe^{2+} Transport and Uncoupled Fluxes. *Pfluegers Arch.* **2006**, *451*, 544–558.

(31) Corbett, T.; Valeriote, F.; LoRusso, P.; Polin, L.; Panchapor, C.; Pugh, S.; White, K.; Knight, J.; Demchik, L.; Jones, J.; Jones, L.; Lowichik, N.; Biernat, L.; Foster, B.; Wozniak, A.; Lisow, L.; Valdivieso, M.; Baker, L.; Leopold, W.; Sebolt., J.; Bissery., M.-C.; Mattes, K.; Dzubow, J.; Rake, J.; Perni, R.; Wentland, M.; Coughlin, S.; Shaw, J. M.; Liverside, G.; Liversidge, E.; Bruno, J.; Sarpotdar, P.; Moore, R.; Patterson, G. Tumor Models and the Discovery and Secondary Evaluation of Solid Tumor Active Agents. *Int. J. Pharmacogn.* **1995**, *33* (Supp.), 102–122.

(32) Corbett, T. H.; Valeriote, F. A.; Demchik, L.; Lowichik, N.; Polin, L.; Panchapor, C.; Pugh, S.; White, K.; Kushner, J.; Rake, J.; Wentland, M.; Golakoti, T.; Hetzel, C.; Ogino, J.; Patterson, G.; Moore, R. Discovery of Cryptophycin-1 and BCN-183577: Examples of Strategies and Problems in the Detection of Antitumor Activity in Mice. *Invest. New Drugs* **1997**, *15*, 207–218.

(33) Corbett, T.; Polin, L.; LoRusso, P.; Valeriote, F.; Panchapor, C.; Pugh, S.; White, K.; Knight, J.; Demchik, L.; Jones, J.; Jones, L.; Lisow, L. In Vivo Methods for Screening and Preclinical Testing; Use of Rodent Solid Tumors for Drug Discovery. In *Anticancer Drug Development Guide*, 2nd ed.; Teicher, B. A., Andrews, P. A., Eds.; Humana Press Inc.: Totowa, NJ, 2004; Chap 6, pp 99−124.

(34) Polin, L.; Valeriote, F.; White, K.; Panchapor, C.; Pugh, S.; Knight, J.; LoRusso, P.; Hussain, M.; Liversidge, E.; Shaw, M.; Golakoti, T.; Patterson, G.; Moore, R.; Corbett, T. H. Treatment of Human Prostate Tumors PC-3 and TSU-PR1 With Standard and Investigational Agents in SCID Mice. *Invest. New Drugs* **1997**, *15*, 99–108.

(35) Polin, L.; Corbett, T. H.; Roberts, B. J.; Lawson, A. J.; Leopold, W. R., III; White, K.; Kushner, J.; Paluch, J.; Hazeldine, S.; Moore, R.; Rake, J.; Horwitz, J. P. Transplantable Syngeneic Rodent Tumors: Solid Tumors of Mice. In *Tumor Models in Cancer Research*, 2nd ed.; Teicher, B. A., Ed.; Humana Press Inc.: Totowa, NJ, 2011; Chapt 3, pp 43−78.

(36) Varela-Moreiras, G.; Selhub, J. Long Term Folate Deficiency Alters Folate Content and Distribution Differently in Rat Tissues. *J. Nutr.* **1992**, *122*, 986–991.